

Magnetic Levitated Drone

“Insector Gadget”

Team Members:

Shantanu Chatterji, Michael Ferguson, Ricardo Hernandez, Tucker Reed, Austin Rolen, Tanner Stokes

MAE 4344: Interdisciplinary Senior Design

Oklahoma State University

May 3, 2019

Table of Contents

1. Design Objective and Constraints	4
2. Team Organization and Project Management	4
3. Concept Design	7
4. Design Calculations	8
Mechanical Subsystem:	8
Electromagnet Subsystem:	9
Electrical Subsystem:	9
Camera Subsystem:	10
Controller Subsystem:	10
5. Component and Material Selection and Sizing	14
Mechanical Subsystem:	14
Electromagnet Subsystem:	16
Electrical Subsystem:	16
Camera Subsystem:	17
6. Instrumentation	17
7. Final Design	22
Mechanical Subsystem:	22
Electromagnet Subsystem:	23
Electrical Subsystem:	23
Controller Subsystem:	24
8. Application of Relevant Standards	24
9. (Prototype) Construction and Testing	25
9.1 (Prototype) Construction	25
9.2 (Prototype) Testing	25
10. Future Work	27

	3
References	28
Appendix	29
A1. Critical Path Chart	29
A2. MATLAB Code Used to Size Electromagnets	30
A3. American Wire Gauge Chart	33
A4. Electromagnetic forces document from Dr. O'Hara	34
A5. Project Cost Analysis	35
A6. Project Standard Operating Procedure	42

1. Design Objective and Constraints

The overall objective of this project was to levitate and maneuver a 1-12mm object in a cubic space with a side length of 20cm, using only magnetism. Ideally this object could be moved at 1-2 m/s. Developing an apparatus to achieve these constraints required a large foundation of understanding and testing. For this reason, we have broke the objective into steps. First, we planned levitate the object at a fixed point. Once we succeed in this, we would begin moving our object in one dimension. After we could move the object in one dimension, we would move to two dimensions, and then three.

In our given timeframe for this project, we chose, in agreement with our client, to focus on achieving movement in one dimension. Such progress would be significant in comparison to current published work. If had early success, and there was sufficient time, we would have continued our work towards movement in further dimensions. Further work will need to continue outside the timeframe of this project.

2. Team Organization and Project Management

Team-customer interaction was a key part to our project. Our customer was our supervising professor, Dr. Faruque. We met with him twice per week to discuss our progress and upcoming work. Each meeting was approximately one hour. We updated him on what our team had done since the last meeting, discussed problems or questions we may have come across, and discussed our plans to continue, both in the short and long term.

Our team was comprised of: a primary supervising professor, Dr. Faruque; an assisting professor, Dr. O'Hara; a project lead and mechanical engineering student, Austin Rolen; three additional mechanical engineering students, Shantanu Chatterji, Tucker Reed, and Tanner Stokes; and two computer engineering students, Michael Ferguson and Ricardo Hernandez. Our team's primary structure for communication can be seen in Figure 1 below. Group members communicated directly with the supervising professors whenever it was reasonable to do so.

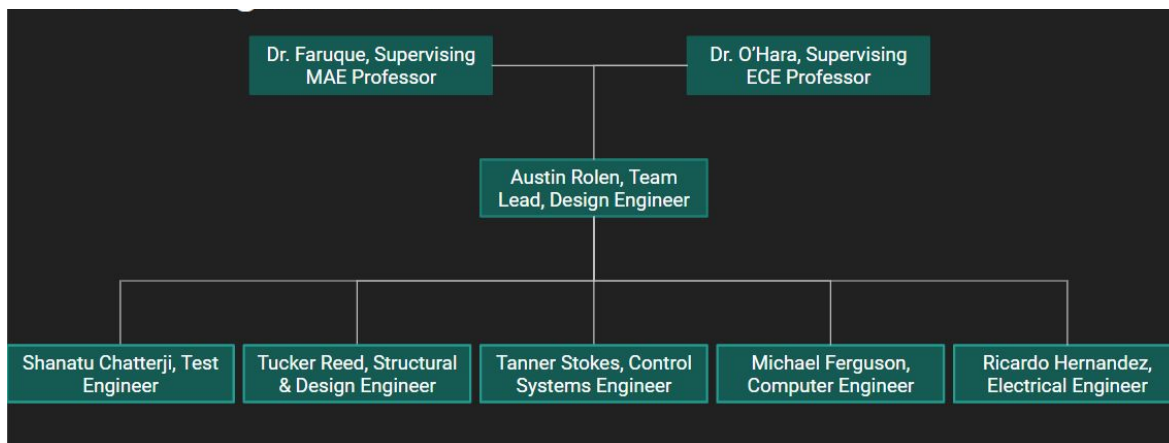


Figure 1: Team communication structure

Our project's original schedule can be seen in both the gantt chart (figure 2) and the project critical path diagram (appendix A1). A legend can be seen in figure 2 for the three types of tasks in the gantt chart. The items in orange are the peer evaluations and engineering leadership series assigned by the interdisciplinary senior design advising professors. The tasks in blue are those directly related to the project. Some of these tasks may be project design, part construction, testing, and part ordering. The last task grouping is for items in green. The green represents project deliverables. These deliverables are documents to support the progress of the project, such as design reports, and the use of the project once completed, such as SOPs, manuals, and decommissioning guides.

The gantt chart below (figure 2) shows the project schedule as it was set at the start of the semester. Due to delays in model testing and unexpected circuitry problems, our progress has not kept pace with our schedule. The blocks in green of the critical path in appendix A1 show our completed tasks, and the blocks in yellow show our ongoing tasks. At this point, we have yet to achieve 0-D levitation. The control loop was closed this week, and our team has not had sufficient time to tune the controller.

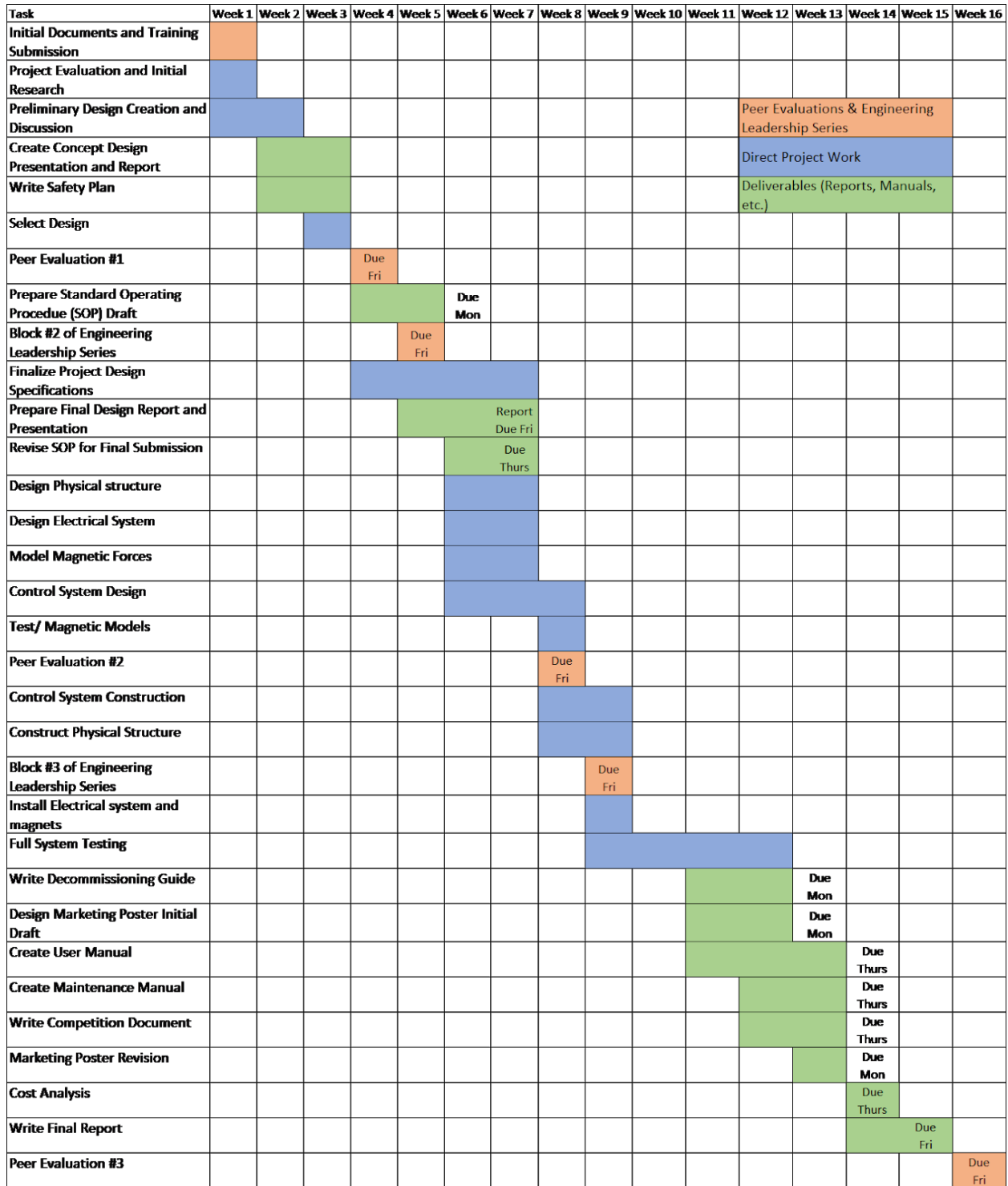


Figure 2: Gantt chart

3. Concept Design

To achieve the design objectives of levitating a ball and maneuvering in 1-dimension using a visual feedback system, a five subsystem approach was taken to effectively organize the design. Each subsystem is interconnected and specifications were dependent on each other. The final concept design consisted of a mechanical system upon which various components would be fastened, the electromagnets in a desired configuration and of proper size, an electrical system to supply the necessary current to each electromagnet, the camera subsystem utilizing a FLEA camera interfacing with MATLAB, and the controller/feedback system that involves a proportional controller for stability based on the positional data provided by the FLEA cameras.

The mechanical subsystem is comprised of a cubic design with additional middle segments across all sides except for one. The side without the extra middle segment was chosen to house the camera backdrop. Such a design provides the greatest flexibility when positioning multiple electromagnets atop and on the side of the structure. The electromagnets and camera can be fastened at almost any point along a segment. The cubic design also provides a structurally sound configuration.

The electrical system needed to achieve a variable current supply. An adjustable voltage regulator was used. The output of the voltage regulator is dependent on a resistor divider that is put along the adjustment pin. One of the resistors is a potentiometer that can interface with the microcontroller. The adjustable voltage output is fed into the gate of a transistor with the collector pin attached to the overall power supply. Based on the gate voltage, a certain current will be conducted through the collector to the emitter. This is the current which passes through the electromagnet.

In designing the electromagnets, a preliminary, analytical model was used with help from Dr. O'Hara. This model gave necessary insight into the controllers and currents needed to achieve levitation. The arrangement of the magnet array also came from this model (figure 3). The three upper electromagnets will maintain levitation of the magnet, and the side electromagnets will be used to produce to 1-D movement.

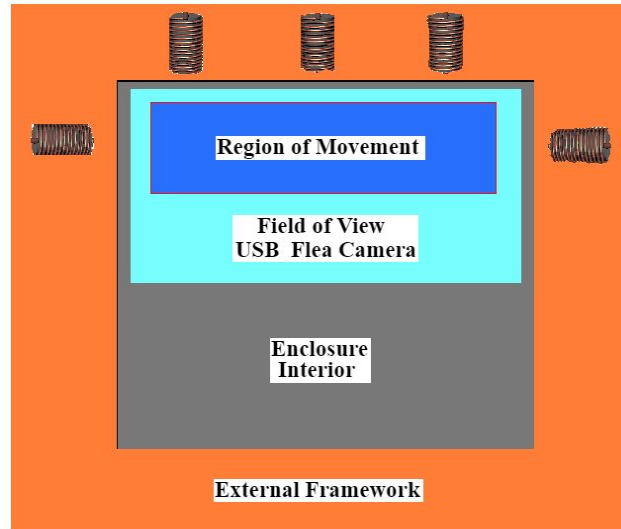


Figure 3: Preliminary sketch of electromagnet configuration

The final two subsystems are the camera and controller subsystems. The camera subsystem utilizes a singular FLEA camera that provides x-z positional data to the controller. Due to the time constraints of the system and the time needed for image processing, the camera uses an area of interest, which can be moved as the magnet moves. The controller uses this visual position data to predict and send the necessary currents to the electromagnets. The controller has a proportional controller, with a derivative controller to soon be added. A lead/lag compensator may be added in the future.

4. Design Calculations

Mechanical Subsystem:

Once an initial structure was determined, 3-D modeling and finite element analysis were used to simulate the loads on the system. Three downward forces of 60N were applied at three points on the top, horizontal segment where the electromagnets were to be fastened. These 60N loads exceeded the expected load of the magnets. This extra load bearing capability in combination with the flexibility of the system will allow for further work and expansion of the project. The two areas of importance in analyzing these forces were the total deformation of the structure and the maximum combined stress. The total deformation came to approximately 0.0274mm, and the total combined stress came to approximately 3.11MPa. The yield strength of the aluminum frame is 280MPa. The safety factor of our frame came out to 45.

Another point of structural consideration was the electromagnet fasteners. Using a static structural simulation, a pressure was applied to the inner face of the fastener that contacts the electromagnet. This was applied as a distributed force to simulate how the fastener would grip the electromagnet. An external force was added to simulate the zip ties that would hold the fasteners in place. With these conditions, the maximum deformation of the fastener was

approximately .02mm, and the total combined stress was approximately 10MPa. Based on these results, a safety factor of 14 was calculated.

Electromagnet Subsystem:

The electromagnet was sized using calculations in a MATLAB script as seen in appendix A2. The goal was to create a magnetic force equalling the force of gravity. An iterative process was used to change the L and N terms until this requirement was met.

$$\text{acc} = F_solenoid(P, I, r_coil, k, L, N, d_wire, Br, V) / \text{mass} + g; \quad (1)$$

P is the point in space as [x y z] in meters, I is the current through the wire in amps, r_core is the radius of the core in meters, k is the core factor measure from testing, L is the number of layers, N is the number of turns of the coil, d_wire is the diameter of the wire in meters, Br is the magnetic field produced by the magnet in tesla, V is the volume of the magnet in meters cubed.

In the code in appendix A2, M is the magnetization of the ball, H is the magnetic field, B is the magnetic flux density, and mu_0 is the permittivity of free space. dH and dB are the respective spatial derivatives of H and B.

Electrical Subsystem:

The key component of the circuit was the coil. The design of the coil dictated how the rest of the circuit needed to be built. Once the coil topology was finalized to five layers and 25 turns each, the amount of voltage could be chosen. Coils have inductance, but it wasn't needed for design calculations since there wouldn't be a frequency of voltage operating across the coil. The main design constraints were the resistance of the coil and the max current to be driven through it. Knowing the gauge of wire thickness wouldn't change the radius of the turn by a large margin, each turn could be seen as an individual circle with the same radius. Using the equation for the circumference of a circle

$$2 * \pi * r \quad (2)$$

with the radius of $r = 0.02\text{m}$, the amount of wire used was roughly 5π meters. To find the resistance of the coil, an American Wire Gauge chart (appendix A3) was used to calculate the resistance per meter. With a coil made from 14 gauge wire, the total resistance came to approximately 0.13Ω . The total voltage drop across the coil at max amperage was calculated using Ohm's Law.

$$V = I * R \quad (3)$$

With a desired current of 5A, a voltage drop of 0.65V was necessary across the coil. Since a mosfet would be used to control the current, there would also be a drop seen across the drain and source terminals. This was also calculated using Ohm's Law since the mosfet has a relatively constant on-resistance. From the datasheet of the BUZ31 mosfet, the resistance was

0.2Ω. This made the total voltage drop across the whole system to be 1.65V. This was the voltage needed to operate the coil correctly.

To connect a digital potentiometer to a mosfet for a complete system, a gate voltage (V_{gs}) to drain current (I_d) relation was to be calculated. Mosfets act differently in two regions that are dependent on the drain voltage (V_{ds}) and the gate threshold (V_{th}) of the chip. If $V_{gs} < V_{ds} + V_{th}$, then the mosfet is operating in a quadratic manner.

$$I_d = k * (V_{gs} - V_{th})^2 / 2$$

$$k = \mu * C_{ox} * W / L$$

If $V_{gs} \gg V_{ds} + V_{th}$ then the mosfet is acting in a linear manner.

$$I_d = k * (V_{gs} - V_{th})$$

The constant k was not given explicitly by the datasheet but by taking data points of the mosfet and fitting a graph on top of the points while altering the value of k close to a rough calculation, values such as 3 and 3.8 were found.

Another design calculation needed was the voltage divider circuit, that would drive the gate voltage of the mosfet to determine the current. To get the range of current from 0 to 5 amps, the gate voltage needed to operate between 2 to 6 volts. To get the highest resolution of selecting the current, the potentiometer needed to operate between these two voltages. Using the voltage divider equation

$$V_{out} = V_{in} \cdot \frac{R_2}{R_1 + R_2} \quad (4)$$

and the constraints of the total resistance of the potentiometer being 20kΩ and the voltage input being 12V, the resistance above the potentiometer would be 30kΩ and the one tied to ground would be 10kΩ.

Camera Subsystem:

The chosen video input device being used had a frame capture rate of 60Hz. This meant that with the MATLAB image processing algorithm fundamentally could not process more than 60 frames per second. This limited the overall processing efficiency. However, it was not necessary to have a resolution higher than that to create a levitating force of magnetism. The Image Acquisition Toolbox in MATLAB utilizes a function called `imfindcircles`(frame, radius[min,max], ...) which has a wide variety of run-times, depending on the parameters used in the function call. As explained later in the 'Instrumentation' section of this document, the run-time was heavily reduced by taking individual frames and cropping them down to a smaller size, reducing the pixels that must be run through the algorithm. Additionally, reducing the range of radii to be searched for within the frame also improved run-time. After optimization due to

lighting, reflection, angle and FOV, the maximum frequency our system's machine-vision interface could operate at 55Hz, given by the equation:

$$T_{\text{total}} = T_{\text{get_frame}} + T_{\text{crop}} + T_{\text{find_circle}} = 7.5\text{ms} + 1\text{ms} + 9.69\text{ms} = 18.19\text{ms} \quad (5)$$

Which corresponds to a frequency of $1/0.01819 = 55\text{Hz}$.

Controller Subsystem:

The control system consists of the controller, computer sensor and actuator. The following gives a discussion on the controller that we originally planned to use in our final design. The sensor is a FLEA camera and is discussed in later sections. The actuator would be a controlled current source for each electromagnet. All of this was planned to be run through MATLAB.

From the various models of electromagnets that were developed by our team and found through research, we were able to study the effects of different control types on the system. Using the simplified model given in the "Undergraduate Research Project" paper, a simple lead compensator controller was shown to levitate a ball about a localized point (Wong). This could also be done for our electromagnet in a similar way. A test would have to be done to measure the change in inductance at a localized point in order to make an accurate model. Problems could occur due to the latency in the camera (16.7 ms), which could be significant enough to make the system unstable. Also, the system model doesn't allow for off center axis movement, only levitation.

Using the model developed by our team, based off of Dr. O'Hara's notes on magnetic forces, levitation, and practical calculations (appendix A4), and the NASA technical report to calculate the force on a magnetized sphere, our team was able to find success in developing proportional and integral controllers for levitation (Simpson). A proportional controller was able to levitate the object, however when a integral control was added to eliminate the steady state error, the oscillations became larger and made the system became unstable (figure 4). Adding a derivative controller was not able to dampen these oscillations (figure 5). Based on these control techniques our team will be able to levitate a ball bearing with some oscillations.

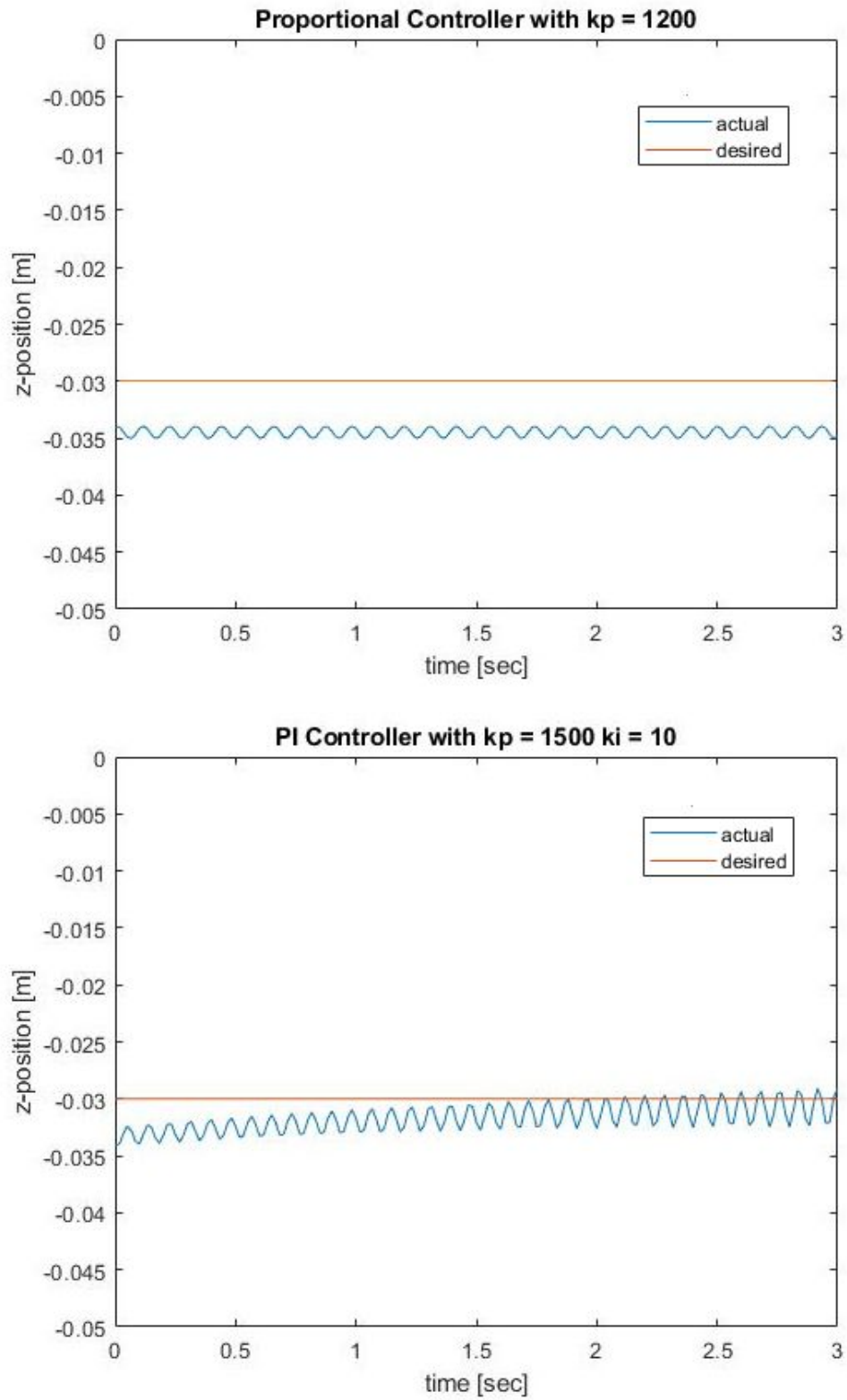


Figure 4: P and PI Controller step responses to a desired point of 3 cm

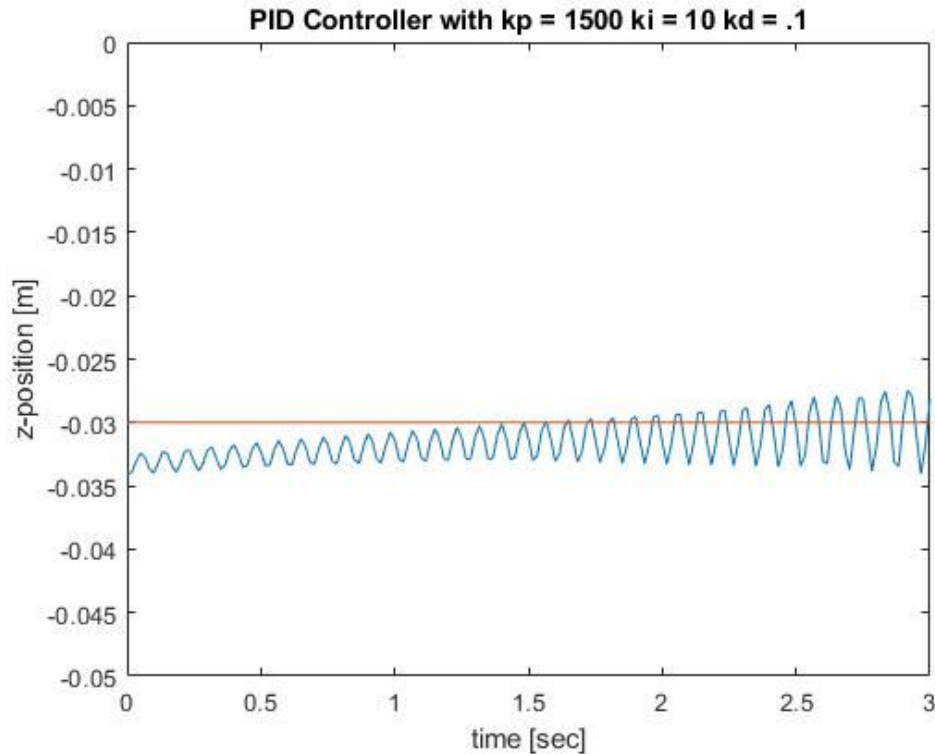


Figure 5: PID Controller step response to a desired point of 3 cm

This provided a starting point for what to use on the actual system to achieve levitation. A couple ways build off this is to add a filter to the camera data to reduce noise and make the precision of the camera better, which will be needed since the proportional gain is so high. The controller could also be gain scheduled at various points to offer the best control of the system at any levitation point.

Going beyond levitation and into directional motion, there were a couple of options to look into

1. Use PID / Lead / Lag compensators (linear controllers) with an inner loop on the levitation and a outer loop on lateral motion (figure 6). It is important to note that the outer loop will be much slower than the inner loop. This may not take into account the exact physics and changing in direction of the various forces affecting the motion, but would be relatively easy to implement.
2. Create a neural network that is trained to model the force vector given a position and electromagnet configuration for a current of 1 Amp and then solve for the current(s) that result in the intended motion of the object. Then control the force vectors directly to align the object to a given path or trajectory. This is similar to a throw and catch between the center axes of two electromagnets

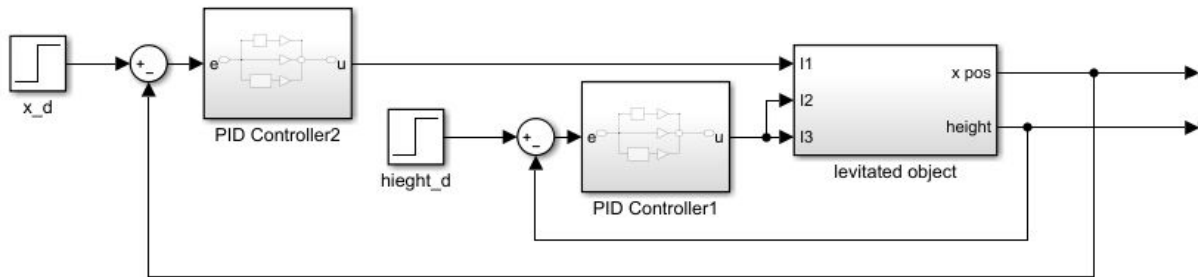


Figure 6: Block Diagram for inner/outer loop controller

Either of these options could work in theory, but more work needs to be done to verify the validity of the models to guarantee they would work on the actual electromagnet. Moving forward, our team planned to use the linear controllers due to familiarity and simplicity in comparison to the neural network. Tuning of the gains would be done on the actual system in order to create the desired response

5. Component and Material Selection and Sizing

Mechanical Subsystem:

For the mechanical structure of the project, we had to consider how the material properties would affect the magnetic component of the system. For this reason, aluminium framing was selected. Specifically, the structural aluminium profiles produced by Minitec. It's unique cross section (figure 7) allows for easy assembly, as well as customization in configuration as needed throughout the testing process, and all future work to be done. Although the current coil size, based on our model, was verified during the testing phase, it is important that the project frame remains flexible in design to allow for future work to be done.

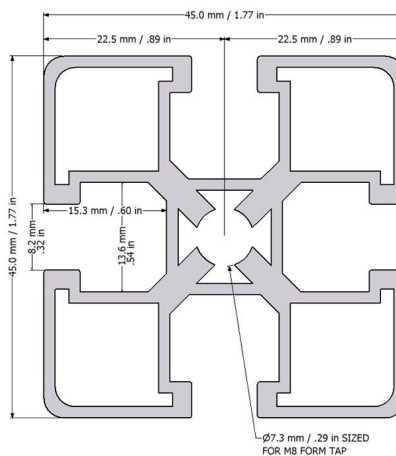


Figure 7: Cross section of aluminium structure

Figure 8 below shows the overall structure of the aluminium frame. The frame has external dimensions of 26cm by 45cm by 49cm.

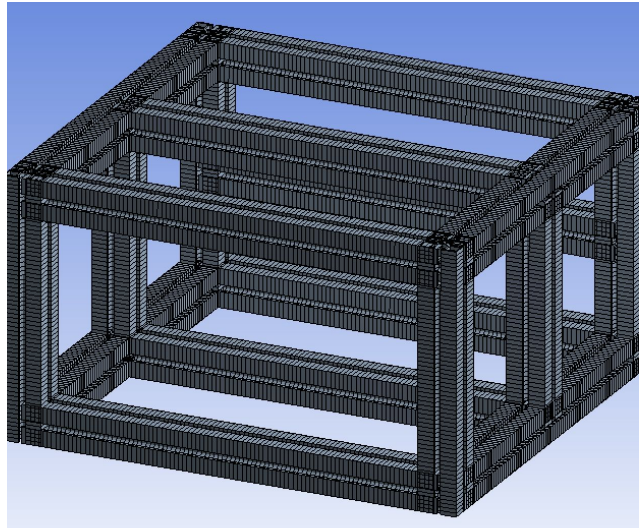


Figure 8: Model of aluminium frame

Figures 9 and 10 depict the two mechanisms used to fasten the electromagnets to the frame. These structures exert a normal force on the electromagnets, which allows the force of static friction to counter the force of gravity. We machined, cut, and bent these fasteners to allow for the best fit with the electromagnets. The current fasteners in use are fashioned to best fit our current electromagnet size, which has a one inch core with 25 turns and five layers of magnet wire, but the fasteners can be further manipulated to account for any changes in electromagnet size that may be the result of future work. In order to ensure the best grip on the electromagnet, and to improve the distribution of the load throughout the fasteners, a zip tie was cinched around the ends of the fasteners.

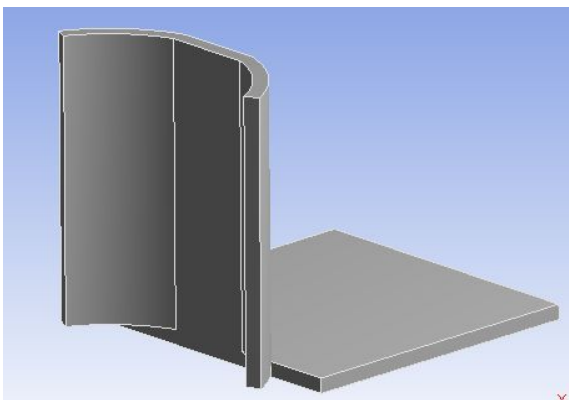


Figure 9: Model of end fastener

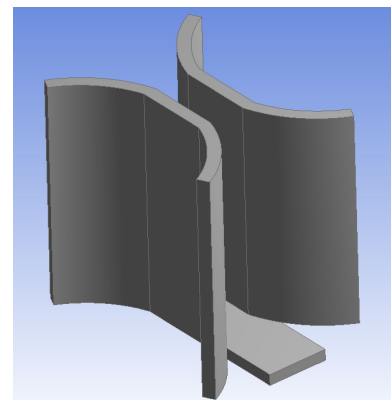


Figure 10: Model of middle fastener

Electromagnet Subsystem:

There were four areas of consideration in selection and sizing of the electromagnet: magnet core diameter, core material, material of object to be levitated, and wire gauge and configuration.

It was important to minimize the diameter of the magnet core so the centers of each electromagnet in the array could be as close as possible to each other. Based on our magnet model we selected a core diameter of one inch. This provided sufficient strength to the magnet, while still keeping the electromagnets relatively close together.

Core material was key to providing the strongest magnetic field possible while keeping the current under 5A. While nickel offers a relative permeability of 100 to 600, iron alloys offer a much higher relative permeability in the range of 5,000 to 200,000, with higher iron percentages having higher permeability. We selected a cold finish, 4130 alloy steel rod which is approximately 98% iron. This was the material with the highest iron content we could find, and could be purchased in one inch diameter rods.

We initially planned to use a ferrous material for the levitated object, but changed to a Neodymium sphere, and more specifically a Neodymium 50 magnet, which was the strongest one we could find. Since we selected a magnetic sphere with a magnetization imposed on it, the relative permeability of the core was no longer directly related to magnet strength; instead, we needed to find the core factor k , which we found through our testing phase. Based on the information we found, it can be assumed a higher relative permeability is associated with a higher k factor, so the core material selection did not need to be changed.

The last material considered for the electromagnet was the wire used to make the coils. We selected 14 gauge magnet wire which is comprised primarily of copper with a very thin coat for insulation. We used 14 gauge based on American Wire Gauge chart (appendix A3), selecting the gauge that would give us a safe range to work with when it comes to varying the current. The size (i.e. the number of turns and layers) of the electromagnets were determined using a MatLab model which we verified in our testing process. Our goal distance for levitation was 3cm, and in order to accomplish this, while minimizing electromagnet diameter and current, we selected an electromagnet comprised of five layers at 25 turns each, and with an operating point around 2 amps. The final size of our electromagnets came out to be 5cm long, and had a diameter of 4 cm.

Electrical Subsystem:

The electrical parts for the subsystem were chosen based off design constraints and efficient power utilization. The BUZ31 mosfet that is used to drive the current was chosen due to its low 0.2Ω on-resistance, thus only dissipating a small portion of the overall power consumption. These mosfets also are able to operate within a wide range of currents that contain the desired currents and allow for a selection of currents based off the gate voltage.

As for the digital potentiometer, there were several constraints that needed to be adjusted for. Most digital potentiometers only allow for small currents to be run through the terminals. With this in mind, a larger resistance allows for that to be attained. Other important aspects were the resolution at which the potentiometer could operate and the communication protocol that controls the setting of the resistance. Knowing these constraints, the AD5293 was chosen. It is a digital potentiometer with a range of 0 to 20k Ω resistance with 1024 unique resistances. It can communicate with a microcontroller over the SPI protocol, a common protocol supported by most commercial microcontrollers. This led to choosing the Arduino Uno, a high-speed microcontroller that has MATLAB support packages that can manipulate the SPI pins found on the board, making the overall system to be operated through MATLAB.

Camera Subsystem:

The MATLAB script runs on a lab computer containing a 2060 RTX graphics card, which was chosen for its speed, to support the computer vision code. MATLAB's Image Acquisition Toolbox supports parallel processing across multiple cores, as well as many of its algorithms being able to run on GPUs as `gpuArray` objects. The main program running in MATLAB is also dependent upon CPU processing speed, which is why we opted to utilize a 4.2GHz Intel CPU. These devices allow our system to operate at the speeds necessary to generate a constant force of magnetic levitation without pulling the target into the electromagnet or dropping the target out of the region of movement.

6. Instrumentation

There are several factors to include when considering what sort of camera will be best suited for the customer's requirements. A high frame rate initially seems to be ideal when considering the design problem, as the more frames per second that can be sent to the Controls subsystem (henceforth sbs.), the faster the magnetostatic algorithm within it can adjust the individual currents, and thus change the magnetic attraction between the target and each solenoid. However, high frame rates will also negatively affect performance; As the number of frames that are processed each second increases, the computing cost required to do so increases linearly as well. Note that a camera's ability to acquire frames at a certain frequency doesn't necessitate each of those frames be utilized during processing, any extra frames are simply wasted. RGB color information can be useful because it allows for more variation in the difference between adjacent regions, however this also causes many popular Computer Vision algorithms to take significantly longer due to the need to convert the image into grayscale for the operations. Considering the various available options, the USB FLEA3 camera manufactured by FLIR was chosen to operate as our video input device. As stated in the concept design section above, only one camera will be utilized to detect movement along the horizontal and vertical axes. In the future, expansion of additional movement axes would require additional cameras.

Table 1: FLEA3 camera properties

Color	Mega-Pixels	Sensor Description	Shutter	Max. Resolution	Max FPS
Mono	1.3MP	e2v EV76C560	Global shutter	1280x1024	60 FPS

In order for the controls sbs. to accurately determine the necessary current required for magnetic levitation, a machine vision interface between the video input device and image processor is required. Depending upon the state of the controls sbs., the target could potentially be located anywhere along the horizontal axis directly below the aligned solenoids; as well as an additional minority height axis. This requires a field-of-view that at least includes the entire length of the interior of which the target could be located (figure 11).

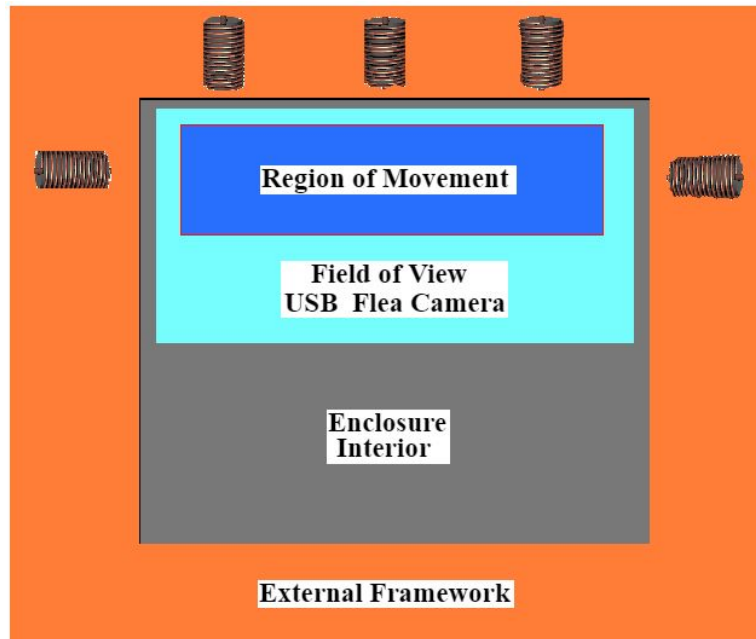


Figure 11: Portrayal of the area seen by the camera located within the enclosure.

Because it is important to have variety in documentation, support, ease of use, and familiarity, the source of our computer vision sbs. has been allocated to MATLAB's Image Acquisition Toolbox. MATLAB fully supports the USB FLEA cameras utilized in the design, and allows for multiple cameras to be utilized in tandem for further expansion. Furthermore, there are many examples already dictating how to detect and track moving objects that will help in the development of the software. Knowing the necessary FOV, we can calculate the distance our camera should be placed based upon the minimum constraints of our Computer Vision algorithm. Experimentally, it was determined that a minimum of 15 pixels should be seen by the

camera in order for an object to be accurately detected. The Flea has a resolution of 1280x1024, and the customer requires objects of at least 1.5mm to be useable.

$$1280 \text{ pixels} / 15 \text{ pixels} = 85.33 \quad (6)$$

$$1.5\text{mm} \cdot 85.33 = 127.995 \text{ mm} = 12.8\text{cm or } 5.03'' \text{ (length)} \quad (7)$$

$$1024 \text{ pixels} / 15 \text{ pixels} = 68.26 \quad (8)$$

$$1.5\text{mm} \cdot 68.26 = 102.39 \text{ mm} = 10.2\text{cm or } 4.01'' \text{ (width)} \quad (9)$$

The length and width found in equations 7 and 9 correspond correctly to the 5:4 aspect ratio of the resolution.

The importance of the machine vision sbs. is in transmitting to the controller a position vector vs. time (X,Y,t) for each frame. The USB FLEA camera operates at a frame rate of 60Hz, which is a period of roughly 16ms. That means that all processing on individual frames, as well as the processing required for the magnetostatic algorithm used in the controller sbs., must be completed within that time to achieve the maximum frame rate possible of the camera. When accounting for the delays in processing inherent to MATLAB's Image Acquisition toolbox, we can see what the actual maximum frame rate achievable will be.

MATLAB's Image Acquisition toolbox contains many different functions that have already been written for the purposes of developing machine vision interfaces. One such function, `imfindcircles(image, [radius_min, radius_max])`, scans an image using a circular Hough transform. A Hough transform is an operation that looks for lines of connected pixels. Because we will already know the exact size of any target that is placed inside the levitation chamber, it will further increase the efficiency of the function call as it is based upon the range of radii that are being looked for.

The following is an example of the `imfindcircle()` operation and output:

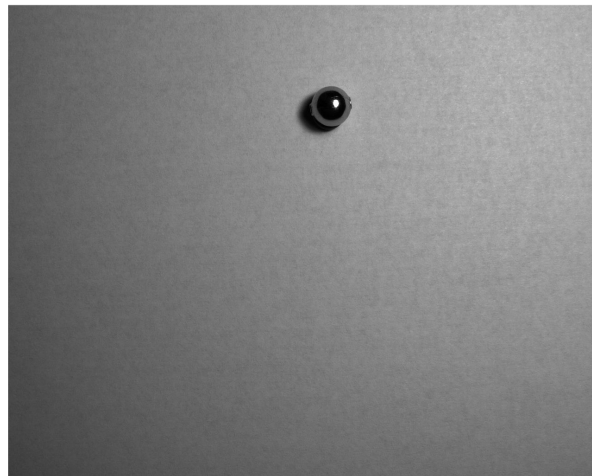


Figure 12: Input image

Figure 12 above shows a single frame taken from the FLEA camera. The object shown is a metallic, spherical bead representing the spherical neodymium magnet to be used in the final product. Which when run with `imfindcircles()` and timed using MATLAB's `tic/toc` feature, it gives a processing time of 605.15ms (figure 13). Note that 605ms is greater than our target processing time of 16ms. Thus we must improve the efficiency in order for this method to work.

```
Processing time for imfindcircles:
Original Frame time: 605.15 ms
Cropped frame time: 64.89 ms
Cropped_Twice frame time: 9.69 ms
```

Figure 13: Initial image processing time

A solution to help `imfindcircles()` complete more quickly is to simply reduce the amount of pixels it is required to check through.

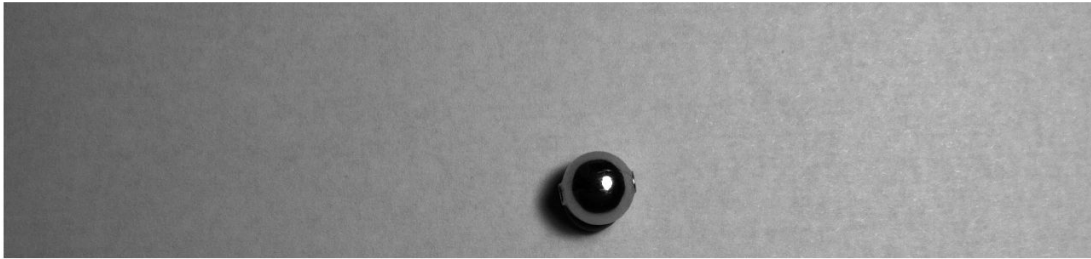


Figure 14: Original frame cropped to the Region of Movement

Cropping the image as seen in figure 14 above increases the processing speed of `imfindcircles()` by an order of magnitude, from 605ms to 65ms. Even still, this is too long for us to fully take advantage of the Flea's 60Hz frame rate, and not frequent enough for the magnetostatic algorithm to levitate the ball.

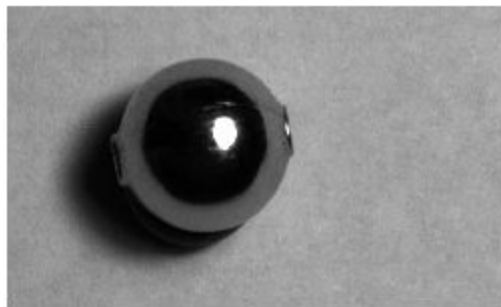


Figure 15 - Region of Movement image cropped, focusing on the target object in order to limit processing duration

By cropping the image to a smaller area (figure 15), centered around the target, the processing speed using `imfindcircles()` can be reduced to a reasonable 9.69ms. It is

algorithmically untaxing to keep track of the specific indices of the cropped image, which itself is then used to determine the center of the target object based upon the last known location of the object and the center (X,Y) position returned from `imfindcircles()`. This method of processing is generally referred to as ROI or Region of Interest processing. Additionally, the time required to crop the image itself is less than 1ms.

```
Cropping times:
1st Crop: 0.91 ms
2nd Crop: 0.19 ms
```

Figure 16: Time required to crop each frame

When the cropped image is run through `imfindcircles()`, the output can be visualized by using the center output and feeding it through the `viscircles(center, radius)` function.



Figure 17: Visualization of the `imfindcircles()` detection of the circular 2D image of the sphere.

Note that `imfindcircles()` is imperfect and can be susceptible to reflections in the image. The red circle shown in figure 17 is actually the spherical reflection and not the outside perimeter of the bead itself. Depending upon the severity of reflection, inaccuracies in data can occur.

Lastly, accounting for the time it takes MATLAB to read each frame from the video input device, we can calculate what actual frequency we can detect the object at using this method.

```
Frame step time 1st: 298.69 ms
Frame step time 2nd: 7.52 ms
Frame step time 3rd: 7.68 ms
Frame step time 4th: 7.12 ms
Frame step time 5th: 7.59 ms
```

Figure 18: Final time required to crop and detect a circle in a series of frames

Initially, there is a setup procedure when asking a video input device for the first frame. This does not occur again unless the video input device is released or disconnected from the computer. Each frame takes roughly 7.5ms to be accepted into MATLAB for data processing. So in total, the overall time required for processing is:

$$T_{\text{total}} = T_{\text{get_frame}} + T_{\text{crop}} + T_{\text{find_circle}} = 7.5\text{ms} + 1\text{ms} + 9.69\text{ms} = 18.19\text{ms} \quad (10)$$

This corresponds to a frequency of $1/0.01819 = 55\text{Hz}$

7. Final Design

Mechanical Subsystem:

The final mechanical system stayed true to the original designs, with a few additions. As can be seen in figure 19 below, an upper platform was added to house conduit boxes for the circuit and microcontroller. Conduit and PVC fittings were used to route electrical wires from the magnets to the circuit.

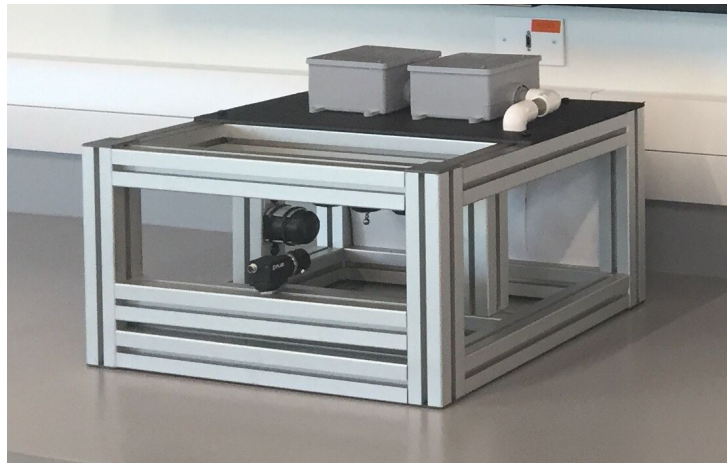


Figure 19: Final mechanical system with other components attached

In order to optimize the camera's performance, a solid, opaque background was added, positioned opposite of the camera (figure 20).



Figure 20: View of system showing background added for the camera

Electromagnet Subsystem:

The final design of the electromagnet was consistent with the original design choices with the exception of the coil geometry. The coil geometry was chosen to be the hexagonal packing (figure 21, right) instead of the square packing (figure 21, left), this would act to minimize the final radius of the coil.

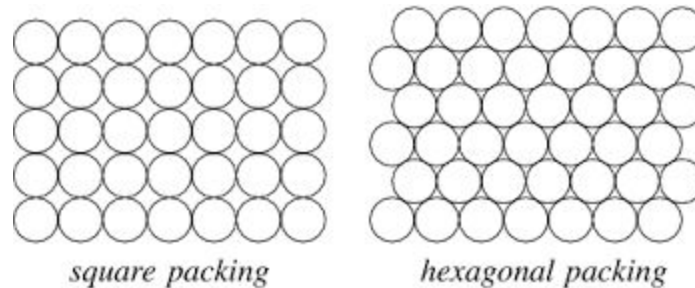


Figure 21: Packing Configuration Types

The hexagonal packing affected the turns per layer we originally designed for. To account for this, each magnet was wound with 28 initial turns and decreased one turn per layer, with the final layer having 24 turns.

Electrical Subsystem:

The final design for the electrical system consisted of three main components: Arduino Uno, AD5293 Digital Potentiometer, and BUZ31 transistor.

The Arduino is primarily used for relaying resistor information from the lab computer running the main MATLAB code to the digital potentiometer that only uses SPI to communicate. Communication was all done through MATLAB since it has its own support package that allows for direct manipulation of the digital pins located on the Arduino board. Several setup functions were used to configure the necessary pins for SPI and for the digital potentiometer to be enabled for register writes. The simple writeRead() function was used to send the 16 bits needed by the AD5293. The first 2 bits being zero for every case, the following 4 being the desired command, and the rest is the data being sent. The digital pin 10 was used as the slave select (SS) or chip select for enabling the AD5293 integrated chip. Pin 11 was used as the serial line for data being sent to the chip or Master Out Slave In (MOSI). Pin 12 is the input pin for data coming from the chip or Master In Slave Out (MISO) and pin 13 is the Slave Clock (SCLK) which determines the speed at which the integrated chip operates. The clock was set to its default frequency of 200kHz. Higher speeds weren't needed since the speed of our system is determined by the camera frame rate. The Arduino also provided power for the logic gates of the chip. The 5V source found on the figure below is the 5V pin of the Arduino.

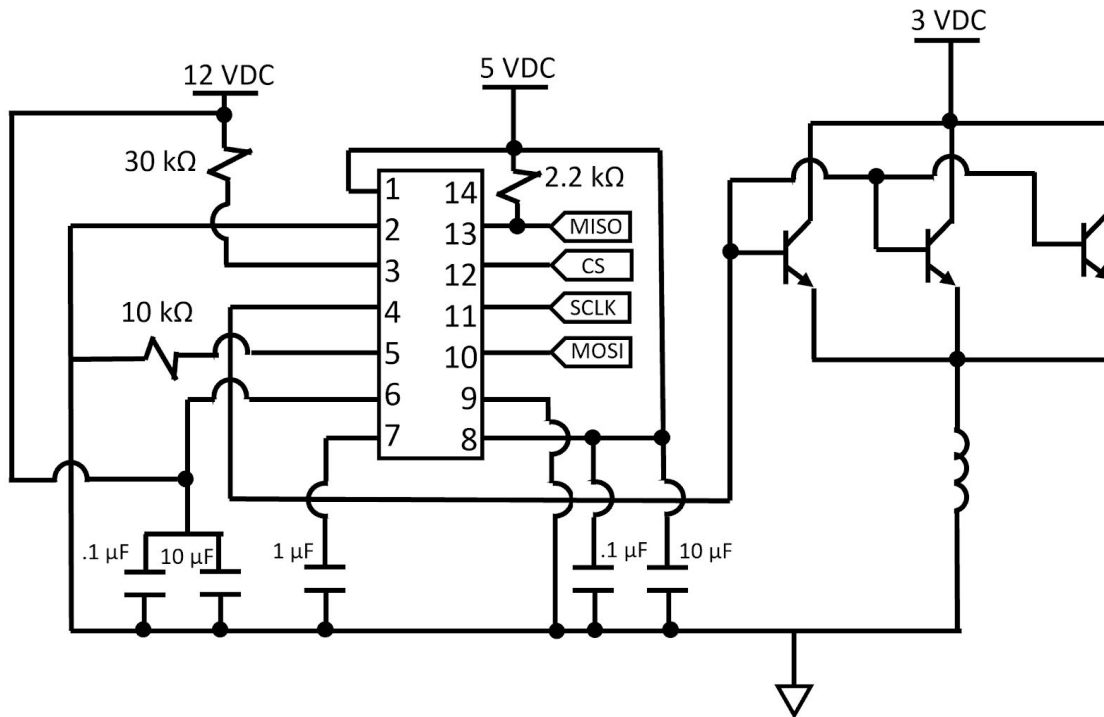


Figure 22: Electrical schematic for current control

The capacitors on pins 6, 7, and 8 are placed so that any fluctuations in the power supply are reduced. The values were determined by the AD5293 datasheet. The voltage output of the chip or pin 4 is fed to the gate of three BUZ31 transistors. This distributes the current or power between the three equally. To allow for the correct operation of the transistors this was needed with the addition of heat sinks. Thermal adhesive was put between the chip case and heat sinks for high thermal transfer.

The 3V power source is supplied by B&K Precision 1901B, a bench AC-DC power supply rated for high currents such as 5A.

Controller Subsystem:

The final design of the controller has not been fully fleshed out. Further steps would need to be employed to tune the gains of the PID controller to achieve the desired response. A P-controller is the starting controller with a k_p value of 1200 as shown in the simulation, then the gains will be tuned from there.

8. Application of Relevant Standards

The goal of this project was to create an apparatus to do something that, to our knowledge, has not been achieved. Due to the nature of such a project, there weren't many standards that applied to our design. The standard that we found to be relevant was the American

Wire Gauge standard. This standard determines the maximum current allowable through various gauges of wire. The diameters of the wire gauges are determined by ASTM B258. A table of these standards can be seen in appendix A3.

9. (Prototype) Construction and Testing

Given the selected building material, the frame construction was completed without issue. The electrical system had a few problems and much debugging was needed to build the circuit and program the Microcontroller. It was suggested to use LabVIEW as opposed to MATLAB and that it would have been more smooth to produce a final product.

9.1 (Prototype) Construction

Construction on this project began with the mechanical portion. We started by screwing the self tapping profile fasteners into each end of the miniTec segments. Two of the miniTec segments needed to be shortened in order to place the side electromagnets as close as possible to the array of electromagnets secured to the top of the mechanical frame.

We then had to cut the steel rods into 5 centimeter segments in order to use them as cores for the electromagnets. Once the cores were cut, five electromagnets were wound with 14 gauge magnet wire, and we used a clamp to ensure the number of turns and layers were as uniform and tight as possible. Once the electromagnets were wound and ready for securement to the frame, the aluminum fasteners (of the dimensions previously mentioned in this document) were bent to best fit our electromagnets. After finishing with the aluminum fasteners, they were secured to the electromagnets with zip ties, one set in a linear array of three electromagnets using two end fasteners and two middle fasteners, and the remaining two electromagnets secured on each end by two end fasteners each. Once the electromagnets were secure in their respective fasteners, we placed the aluminum nuts through their respective holes on the fasteners, and then loosely connected the aluminum nuts to the other side. From there, we slid the the secured electromagnets into the t-slots of the miniTec segments and then tightened them into place. Finally, once the electromagnets were secured to the correct segments, we assembled the miniTec segments by sliding them to the correct spot, in accordance with the final design, and then tightened them into place with an allen key. Before the final couple of segments could be slid into place, the camera mount, which is comprised of a bolt and two washers, had to be slid into the t-slots.

Once all the segments were together, only a few adjustments to certain segments were made to ensure the electromagnets were as close as possible, while still at the best position possible for our target object to be picked up by the FLEA camera. After tightening everything down, the only thing left to do was add the end caps to the 8 ends where the cross-section of the miniTec segments were visible and then the mechanical construction was completed.

9.2 (Prototype) Testing

In order to test the prototype, we separately tested the all of the subsystems and then combined them to close the loop. testing of the various subsystems are mentioned in the sections above so it will be discussed briefly here. The camera was tested by setting a small ball on piece of paper and taking measurements of the object to measure the variance of the center calculation. It was found that the variance of the calculation was less than a pixel, and when taking into account the ball will be approximately 12.5 cm away, the variance would be .012 mm on the center of the ball. This is expected since camera and computer vision systems are very precise. Next, testing of the electrical system took place, where a multimeter was used to measure the current through the coil and MATLAB commands sent the desired current. These two were compared and seen to be very similar. This means that we can measure the position of the ball and control the current through the coil, meaning the loop was ready to be closed.

Once these subsystems were checked, the loop was closed and controller testing began. The model gave a starting point for the controller at around 1200, but this was using the difference in meters so converting to millimeters, the proportional gain would be 1.2. Starting at this gain value and a desired position of 30 mm, we iteratively attempted levitation. a table of the best attempts are shown below with a graph of the control current versus time, which shows the levitation of the ball for approximately 0.5 seconds. the increasing magnitude shows the system is still unstable. Table 2 below shows that a gain schedule could possibly be performed to change the controller based on the desired position, causing small movement up and down on the center axis.

Table 2: Current system gain schedule

kp	3.045	3.07	3.093
deszpos [mm]	24.75	24.8	24.85

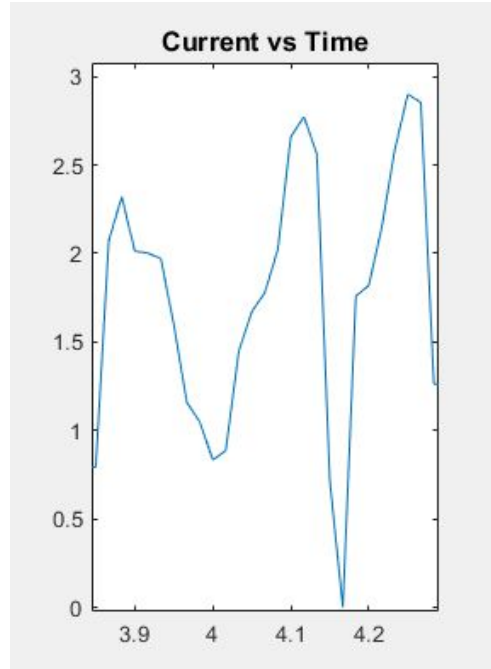


Figure 23: Current [A] (y-axis) vs. Time [sec] (x-axis) for best levitation attempt

10. Future Work

The future work for this project largely follows the original critical path in appendix A1. The final control parameters for 0-D levitation need to be determined. From there, the project can be expanded to attempt 1-D movement. Currently, only the center electromagnet has a completed circuit. Circuits will need to be made and installed for the other four magnets in order to move forward to 1-D movement. Relays will need to be added to control the current to each electromagnet circuit. Expansion to 2-D and 3-D movement would require the addition of more electromagnets and circuits.

At the moment, the project utilizes a proportional controller, with a derivative controller to soon be added. As more magnets are added, the type of controller may need to be changed. Depending on how the addition of multiple electromagnets affects the magnetic field, a nonlinear controller may need to be added.

References

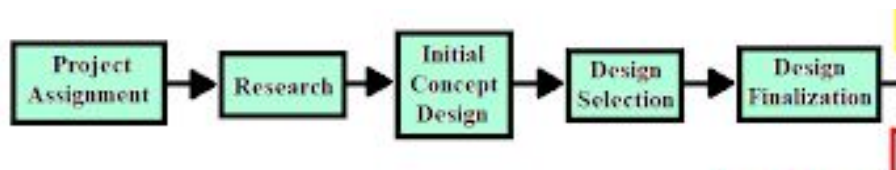
Simpson, James C, et al. Simple Analytic Expressions for the Magnetic Field of a Circular Current Loop.

Wong, T. H. "Design of a Magnetic Levitation Control System???An Undergraduate Project." *IEEE Transactions on Education*, E-29, no. 4, Nov. 1986, pp. 196–200., doi:10.1109/te.1986.5570565.

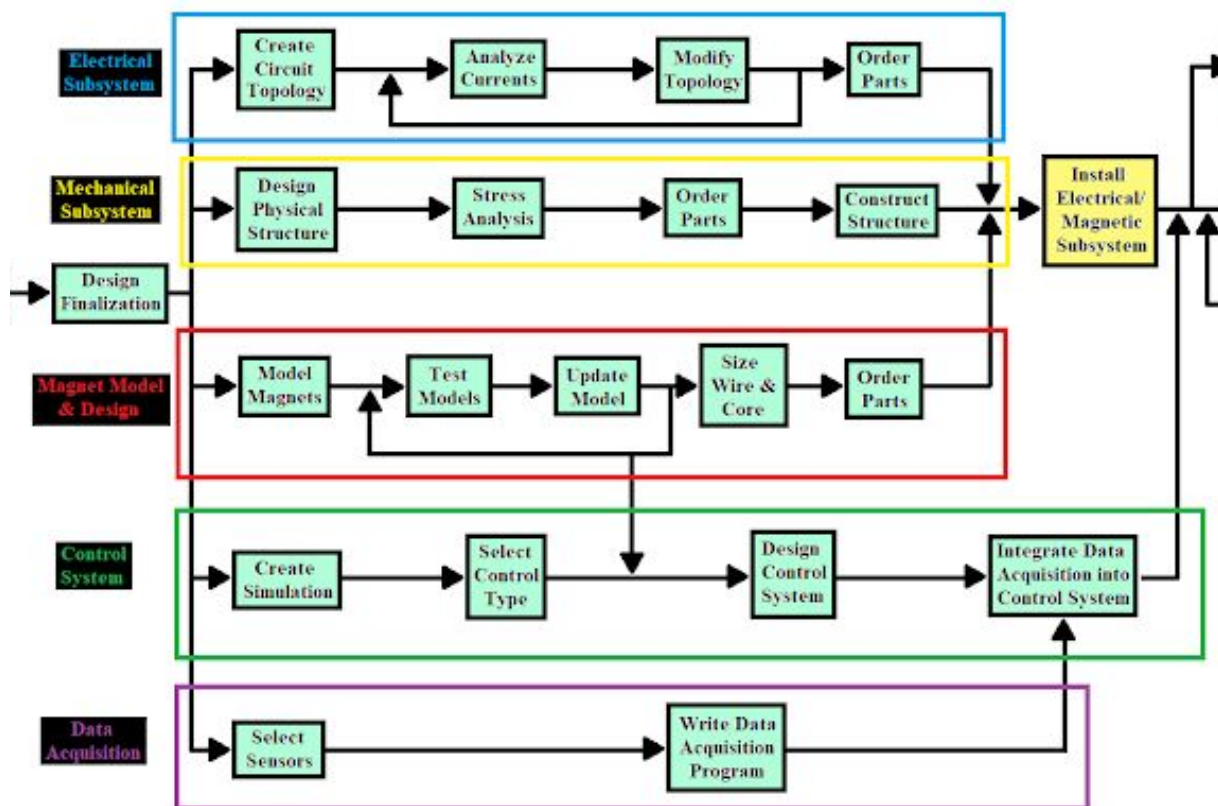
Appendix

A1. Critical Path Chart

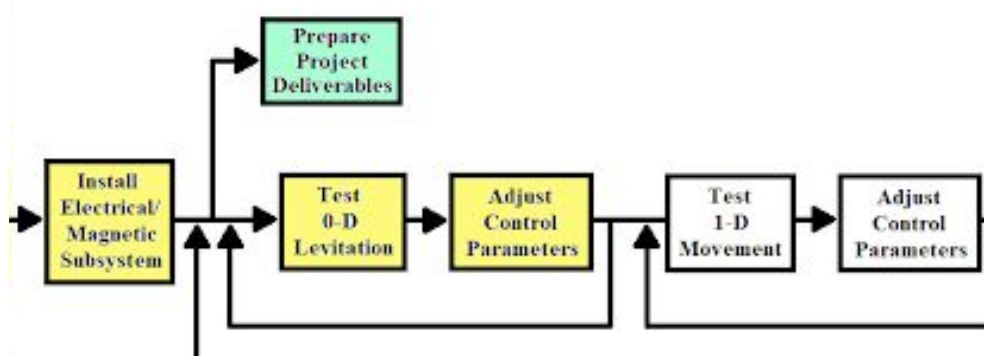
Part 1:



Part 2:



Part 3:



A2. MATLAB Code Used to Size Electromagnets

```

function [B, dB] = B_solenoid(P,I,r_core,k,L,N,d_wire)
    B = [0,0,0];
    dB = zeros(3);
    for j = 1:L
        if mod(j,2) == 1
            P_i = P;
        else
            P_i = P+[0, 0, d_wire*0.5]; %circle packing configuration increase radius
        end
        for i = 1:N
            [Bloop, dB_loop] = B_loop(P_i,I,r_core);
            % dB is calculated but is unused in the solenoid as the force
            % calculation is what uses the derivatives
            dB = dB + dB_loop;
            B = B + Bloop;
            P_i = P_i + [0,0,d_wire];
        end
        r_core = r_core+d_wire*cos(pi/6); %increases radius by d*cos(pi/6)
    end
    B = B*k;
    dB = dB*k;
end

```

```

function F = F_solenoid(P,I,r_core,k,L,N,d_wire, Br, V)
    mu_0 = 1.25663706144*10^-6;
    [B, dB] = B_solenoid(P,I,r_core,k,L,N,d_wire);
    H = (1/mu_0)*B;
    dH = (1/mu_0)*dB;

    M = Br*H./norm(H);

    M_del_H = [M(1)*dH(1,1)+M(2)*dH(1,2)+M(3)*dH(1,3);
               M(1)*dH(2,1)+M(2)*dH(2,2)+M(3)*dH(2,3);
               M(1)*dH(3,1)+M(2)*dH(3,2)+M(3)*dH(3,3)];

    F = V*M_del_H;
end

```

```

function [B,B_diriv] = B_loop(P,I,a)
    % calculates magnetic flux density and spatial derivatives of a electromagnet
    % at a point with given current and radius of coil
    mu_0 = 1.25663706144*10^-6;
    x = P(1); y = P(2); z = P(3);

    % intermediate variables as shown in NASA Simple Analytic
    % Expressions for the Magnetic Field of a Circular Current Loop
    rho = sqrt(x^2+y^2);
    r = sqrt(x^2+y^2+z^2);
    alpha = sqrt(a^2+r^2-2*a*rho);
    beta = sqrt(a^2+r^2+2*a*rho);
    k = sqrt(1-(alpha^2/beta^2));
    lambda = x^2-y^2;
    C = mu_0*I/pi;

    %elliptic E and K integrals evaluated a k^2
    E = ellipticE(k^2);
    K = ellipticK(k^2);

    % Calculation of Flux density as shown in NASA Simple Analytic
    % Expressions for the Magnetic Field of a Circular Current Loop
    % section 3: CARTESIAN COORDINATES
    Bx = (C*x*z/(2*alpha^2*beta*rho^2))*((a^2+r^2)*E-K*alpha^2);
    By = (C*y*z/(2*alpha^2*beta*rho^2))*((a^2+r^2)*E-K*alpha^2);
    Bz = (C/(2*alpha^2*beta))*((a^2-r^2)*E+K*alpha^2);

    if isnan(Bx)
        Bx = 0;
    end
    if isnan(By)
        By = 0;
    end

    B = [Bx, By, Bz];

```

```

% calculation of spatial derivative

den = 2*alpha^4*beta^3*rho^4;

dBx_dx = C*z/den*((a^4*(-lambda*(3*z^2+a^2)+rho^2*(8*x^2-y^2))- ...
    a^2*(rho^4*(5*x^2+y^2)-2*rho^2*z^2*(2*x^2+y^2)+3*z^4*lambda)- ...
    r^4*(2*x^4+lambda*(y^2+z^2)))*E+ ...
    (a^2*(lambda*(a^2+2*z^2)-rho^2*(3*x^2-2*y^2))+ ...
    r^2*(2*x^4+lambda*(y^2+z^2)))*alpha^2*K);

dBx_dy = C*x*y*z/den*((3*a^4*(3*rho^2-2*z^2)+r^4*(2*r^2+rho^2)- ...
    2*a^6-2*a^2*(2*rho^4-rho^2*z^2+3*z^4))*E+ ...
    (r^2*(2*r^2+rho^2)-a^2*(5*rho^2-4*z^2)+2*a^4)*alpha^2*K);

dBx_dz = C*x/den*((rho^2-a^2)^2*(rho^2+a^2)+ ...
    2*z^2*(a^4-6*a^2*rho^2+rho^4)+z^4*(a^2+rho^2))*E- ...
    ((rho^2-a^2)^2+z^2*(rho^2+a^2))*alpha^2*K);

dBy_dx = dBx_dy;

dBy_dy = C*z/den*((a^4*(lambda*(3*z^2+a^2)+rho^2*(8*y^2-x^2))- ...
    a^2*(rho^4*(5*y^2+x^2)-2*rho^2*z^2*(2*y^2+x^2)-3*z^4*lambda)- ...
    r^4*(2*y^4-lambda*(x^2+z^2)))*E+ ...
    (a^2*(-lambda*(a^2+2*z^2)-rho^2*(3*y^2-2*x^2))+ ...
    r^2*(2*y^4-lambda*(x^2+z^2)))*alpha^2*K);

dBy_dz = C*y/den*((rho^2-a^2)^2*(rho^2+a^2)+ ...
    2*z^2*(a^4-6*a^2*rho^2+rho^4)+z^4*(a^2+rho^2))*E- ...
    ((rho^2-a^2)^2+z^2*(rho^2+a^2))*alpha^2*K);

dBz_dx = dBx_dz;

dBz_dy = dBy_dz;

dBz_dz = C*z/(2*alpha^4*beta^3)*((6*a^2*(rho^2-z^2)-7*a^4+r^4)*E+ ...
    alpha^2*(a^2-r^2)*K);

B_diriv = [dBx_dx dBx_dy dBx_dz;
            dBy_dx dBy_dy dBy_dz;
            dBz_dx dBz_dy dBz_dz];

for i = 1:3
    for j = 1:3
        if isnan(B_diriv(i,j))
            B_diriv(i,j) = 0;
        end
    end
end
end
end

```

A3. American Wire Gauge Chart

AWG	Diameter (mm)	Diameter (in)	Square (mm ²)	Resistance Copper (ohm/1000m) <small>(ohm/1000ft)</small>	Typical Max. Current Load Ratings - Copper (amps) ¹⁾					
					Single Core	Multicore				
						up to 3 cores	4 - 6 cores	7 - 24 cores	25 - 42 cores	43 and above
40	0.08	.	0.0050	3420						
39	0.09	.	0.0064	2700						
38	0.10	0.0040	0.0078	2190						
37	0.11	0.0045	0.0095	1810						
36	0.13	0.0050	0.013	1300						
35	0.14	0.0056	0.015	1120						
34	0.16	0.0063	0.020	844						
33	0.18	0.0071	0.026	676						
32	0.20	0.0080	0.031	547						
30	0.25	0.010	0.049	351						
28	0.33	0.013	0.080	232						
27	0.36	0.014	0.096	178						
26	0.41	0.016	0.13	137						
25	0.45	0.018	0.16	108						
24	0.51	0.020	0.20	88	3.5	2	1.6	1.4	1.2	1.0
22	0.64	0.025	0.33	52	5.0	3	2.4	2.1	1.8	1.5
20	0.81	0.032	0.50	34	6.0	5	4.0	3.5	3.0	2.5
18	1.0	0.040	0.82	22	9.5	7	5.6	4.9	4.2	3.5
16	1.3	0.051	1.3	13	15	10	8.0	7.0	6.0	5.0
14	1.6	0.064	2.1	8.5	24	15	12	10	9.0	7.5
13	1.8	0.072	2.6	6.8						
12	2.1	0.081	3.3	5.4	34	20	16	14	12	10
10	2.6	0.10	5.3	3.4	52	30	24	21	18	15
8	3.3	0.13	8.3	2.2	75	40	32	28	24	20
6	4.1	0.17	13.3	1.5	95	55	44	38	33	27
4	5.2	0.20	21.2	0.80	120	70	56	49	42	35
3			26.7		154	80	64	56	48	40
2	6.5	0.26	33.6	0.50	170	95	76	66	57	57
1	7.4	0.29	42.4	0.40	180	110	88	77	66	55
0 (1/0)	8.3	0.33	53.5	0.31	200					
00 (2/0)	9.3	0.37	67.4	0.25	225					
000 (3/0)	10.4	0.41	85.0	0.20	275					
0000 (4/0)	11.7	0.46	107	0.16	325					
250			127		345					
300			152		390					
400			178		415					

https://www.engineeringtoolbox.com/wire-gauges-d_419.html

A4. Electromagnetic forces document from Dr. O'Hara

Begins on the following page

A5. Project Cost Analysis

Prototype System Costs:

All parts are priced without tax. Labor costs are estimated at \$40/hour shop labor rate and \$75/hour engineering and marketing labor rate.

Bill of Materials

Below is the bill of materials for the prototype. We were given a budget of \$2,000. Our total cost was \$1,197.35.

Supplier	Part Description	Part Number	Quantity	Cost/Unit	Cost/all units	Shipping
MiniTec	26 cm Alum. Frame Segment	20.1063	6	\$8.45	\$50.72	-
MiniTec	40 cm Alum. Frame Segment	20.1063	7	\$3.72	\$26.07	-
MiniTec	36 cm Alum. Frame Segment	20.1063	4	\$7.07	\$28.26	-
MiniTec	Profile Fasteners	21.0818	26	\$4.80	\$124.80	-
MiniTec	End Caps	22.1004	8	\$1.20	\$9.60	-
MiniTec	Labor to Cut Alum. Segments	25.1094	-	\$51.00	\$51.00	-
Lowes	4 ft x 1.5 in x 1/16 in aluminum flat	Item #215983, Model #11323	3	\$5.93	\$17.79	-
Pro-Bolt	Aluminium Dome Head Bolt M6 x (1.00mm) x 10mm Pack x 10	FB610-10	2	\$13.78	\$27.56	\$7.50
Pro-Bolt	Aluminium Full Nuts M6 Pack x 10	FN6-10	2	\$9.43	\$18.86	\$7.50

Bulk Wire	14 AWG 1 lb Magnetic Wire	Wire-MW-14- 1	1 lb	\$26.59	\$26.59	\$14.49
Bulk Wire	12 AWG 1 lb Magnetic Wire	Wire-MW-12- 1	1 lb	\$26.17	\$26.17	
Bulk Wire	10 AWG 1 lb Magnetic Wire	Wire-MW-10- 1	1 lb	\$25.60	\$25.60	
Super Magnet Man	1mm Neodymium Sphere Magnet	SP0100-50	1	\$12.95	\$12.95	\$8.29
Super Magnet Man	5mm Neodymium Sphere Magnet	SP0500-25	1	\$12.95	\$12.95	
Super Magnet Man	8mm Neodymium Sphere Magnet	SP100352	5	\$1.50	\$7.50	
Digi-Key Electronic s	Beaglebone Black MCU	BBB01-SC-50 5-ND	1	\$62.38	\$62.38	\$8.99
Digi-Key Electronic s	Linear Voltage Regulator IC Positive Adjustable 1 Output 5A	LMS1585ACS X-ADJ/NOPB CT-ND	5	\$2.73	\$13.65	
Digi-Key Electronic s	IGBT 250V 41A 150W Surface Mount TO-252	FGD3325G2-F 085DKR-ND	5	\$3.07	\$15.35	
Digi-Key Electronic s	Digital Potentiometer 20k Ohm 1 Circuit 1024 Taps SPI Interface 14-TSSOP	AD5293BRUZ -20-RL7CT-N D	5	\$6.88	\$34.40	

Digi-Key Electronic s	TSSOP-14 TO DIP-14 SMT ADAPTER	PA0033-ND	10	\$3.69	\$36.90	
Digi-Key Electronic s	TO-252 DPAK TO DIP-6 SMT ADAPTER	PA0183-ND	10	\$3.69	\$36.90	
Digi-Key Electronic s	Diode Standard 45V 20A (DC) Surface Mount DPAK	497-18030-1- ND	10	\$0.63	\$6.32	
Digi-Key Electronic s	Zener Diode 12V 500mW ±5% Surface Mount SOD-123	MMSZ5242B- TPMSCT-ND	5	\$0.22	\$1.10	
Digi-Key Electronic s	TO-263-3 DDPAK/D2PAK TO DIP-6 SM	PA0184-ND	10	\$4.19	\$41.90	
Sparkfun	N-Channel MOSFET 60V 30A	COM-10213	15	\$0.95	\$14.25	\$6.66
Mouser Electronic s	PCBs & Breadboards 4Pk SchmartPatch for 0603/0805/SOD1 23	203-0001-01	1	\$15.00	\$15.00	\$7.99
Amazon	100pcs Male Header Pins, Lystaii Straight Single Row 40 Pin 0.1 Inch	-	1	\$7.49	\$7.49	\$11.98
Amazon	Chanzon 12V 5A 60W AC DC	-	1	\$15.84	\$15.84	

	Power Supply Adapter					
Amazon	ELEGOO 130pcs Solderless Flexible Breadboard Jumper Wires Male to Male for Arduino Breadboard	-	1	\$6.99	\$6.99	
Online Metals	Cold Finish Alloy Steel Round Bar 4130 (1")	#7368	3	\$13.98	\$41.94	\$21.10
Pro-Bolt	Aluminium Socket Cap Bolt M6 x (1.00mm) x 12mm Pack x 10	PB612-10	1	\$11.17	\$11.17	\$7.50
Bulk Wire	14 AWG 5 lb Magnetic Wire	Wire-MW-14-5	5 lbs	\$102.89	\$102.89	\$16.32
Bulk Wire	14 AWG 1 lb Magnetic Wire	Wire-MW-14-1	1 lbs	\$26.59	\$26.59	
Digi-Key Electronics	BREADBOARD GENERAL PURPOSE PTH	1738-1001-ND	10	\$2.99	\$29.90	\$29.99
Digi-Key Electronics	Bipolar (BJT) Transistor NPN 45V 100mA 300MHz 625mW Through Hole TO-92	BC547B-APM SCT-ND	7	\$0.48	\$3.36	
Digi-Key Electronics	RELAY GEN PURPOSE SPST 5A 12V	255-3589-ND	7	\$1.90	\$13.30	

Digi-Key Electronic s	IGBT 600V 9A 25W Through Hole TO-220FP	497-5114-5-N D	20	\$1.30	\$26.00	
Digi-Key Electronic s	Heat Sink Assorted (BGA, LGA, CPU, ASIC...) Aluminum Alloy Top Mount	AE11388-ND	20	\$0.46	\$9.24	
Digi-Key Electronic s	Thermal Pad Gray 228.60mm x 228.60mm Square Tacky - Both Sides	926-1128-ND	2	\$8.63	\$17.26	

Labor Costs

The prototype production time also includes initial research and brainstorming conducted at the start of the semester. With a total labor time of 575.5 engineering and marketing hours and 47.5 shop hours, our total labor cost comes to \$45,062.50.

Work Type	Labor Cost	Total Hours	Total Cost
Mechanical Structure Design	\$75/hour	23	\$1,725
Control System Design	\$75/hour	39	\$2,925
Electrical System Design	\$75/hour	40	\$3,000
Mechanical Prototype Construction	\$40/hour	27.5	\$1,100
Electrical Prototype Construction	\$40/hour	20	\$800

Control Software Development	\$75/hour	27.5	\$2,062.50
Image Acquisition and Processing Development	\$75/hour	61	\$4,575
Initial Research/Training	\$75/hour	171.5	\$12,862.50
Magnetic Field Modeling and Verification	\$75/hour	63	\$4,725
Documentation package	\$75/hour	128.5	\$9,637.50
Marketing materials development	\$75/hour	22	\$1,650

Maintenance Costs (5 years):

The system maintenance costs are separated into energy consumption costs and direct system maintenance.

System Maintenance

Our system should not require regular maintenance. The most that should be needed in to check every six months that all bolts are tight. This will only take one person, and they will spend approximately 30 minutes per year. At \$70/hour for maintenance personnel, this results in \$175 in regular maintenance costs over five years.

Energy Consumption

Three Main Power Consumers:

1. Personal Computer - Contains all code and supplies power to FLEA camera and Arduino
2. DC Power Supply - Supplies current to coils (in this case a single coil)
3. 12V AC-DC Adapter - Supplies voltage to voltage divider

Personal Computer:

Using an online calculator that takes in as inputs all the individual components that construct the PC, for one hour at max performance the PC consumes 500 watts of power. In reality it will be using less power since its assuming it's running an intensive 3d modeling program but the computer will be capturing 60 fps of video while running computations to identify an object.

DC Power Supply:

At max settings, the power supply will be supplying 5 amps at 3 volts. Using the simple power formula $P = VI$, we can see that it will be supplying 15W of power.

12V AC-DC Adaptor:

This adapter is rated for 5A but will only using a fraction. It will be plugged in to supply a voltage to the gate of a series of MOSFETS which draw current in the microamps thus negligible. The majority of current will be going through the resistors that make the voltage divider. Using the simple power formula again, $P = V^2 / R$, the power consumption will be around 2mW.

Total Power:

$$500W + 15W + 0.002W = 500.002W = 105W$$

For 600 hours of use,

$$500W * 600 \text{ Hrs} / 1000 = 300 \text{ kWh}$$

The current rate cost per kWh is \$0.03467/kWh during peak season from [PSO](#). From there, at 300kWh/year for 5 years, our energy consumption costs come to \$52.

A6. Project Standard Operating Procedure

Begins on the following page

A7. Final Code

```

clc; clear; close all;

%-----Constants-----

% Camera object
flea_camera = imaq.VideoDevice('pointgrey');

% Mosfet parameters
k = 2.8;
k1 = 2.76;
Vt = 3;
Vt1 = 3.5;

%Desired Position
ypixel_22mm = 22 / .071428 + 120; % zpos = (previous_center(2)-120)*.071428;

% AD5293 Digital Potentiometer Commands
writeCmd = bin2dec('0000 0100');
firstPrepCmd = bin2dec('0001 1000');
secPrepCmd = bin2dec('0000 0010');
firstImpedCmd = bin2dec('1000 0000');
secImpedCmd = bin2dec('0000 0001');
firstReadCmd = bin2dec('0000 1000');
secReadCmd = bin2dec('0000 0000');

```

```
%Camera constants
global capture_data;
global finished;
global highlights;
capture_data = true;
finished = false;
highlights = true;

%controller paramaters
deszpos = 25; %3 cm

%plotting arrays
lastsec = 10;
zpos_arr = zeros(lastsec*60,1);
Id_arr = zeros(lastsec*60,1);
t = 1/60:1/60:lastsec;
i = inf;

%-----Arduino Set-Up-----

a = arduino('COM8', 'Uno', 'Libraries', 'SPI');

% Configure the spi object
spi = spidev(a, 'D10', 'Mode', 1, 'BitOrder', 'msbfirst', 'Bitrate', 200000);
```

```

% Enable RDAC register writing
data = writeRead(spi, [24 2], 'uint8');

% Set SDO pin to high impedance
data = writeRead(spi, [firstImpedCmd secImpedCmd], 'uint8'); %0x8001 command
data = writeRead(spi, [0 0], 'uint8'); %followed by NOP command sets
high impedance

%-----

%Grab the first frame for setup and crop.
frame = step(flea_camera);
%cropped = imcrop(frame,[(1280/2-110),120,305,1024]); column
cropped = imcrop(frame,[(1280/2),ypixel_22mm-100,100,200]); %small ROI

%Create the GUI.
gui = figure;
set(gui, 'Position', get(0,'Screensize')); % Maximize figure.
set(gui,'WindowKeyPressFcn',@KeyPressFcn);

%Create the frame preview.
hAxes_f = subplot(2,3,[1,2,4,5]);
hFrame = imshow(frame,'Parent',hAxes_f);
yline(hAxes_f,550,'-y');
yline(hAxes_f,320,'-b');
xline(hAxes_f,670,'-w');
axis on;
title('Video Input Frame','FontSize',12);

```

```

%Create the region of interest.

hAxes_c = subplot(2,3,3);
hCropped = imshow(cropped,'Parent',hAxes_c);
axis on;
title('Region of Interest','FontSize',12);

%yline(hAxes_c,200,'-.b');
%yline(hAxes_c,ypixel_15mm,'-.w');
%yline(hAxes_c,430,'-.y');

previous_center = [1280/2,1024/2];
%hCircle =
rectangle(hAxes_c,'Position',[(previous_center(1)-44),(previous_center(2)-44),88,88],'Curvature'
,[1,1],'FaceColor','none');
hRect =
rectangle(hAxes_f,'Position',[(previous_center(1)-110),120,305,1024],'FaceColor',[0 1 1 0.2]);

%create current graph
hAxes_g = subplot(2,3,6);
hPlot = plot(t,Id_arr,'Parent',hAxes_g);
axis([0 lastsec 0 5]);
title('Current vs Time','FontSize',12);

while(~finished)
    while (capture_data)
        %Get the next frame from the camera.
        tic;

```

```

frame = step(flea_camera);
frametime = toc;

%Update the frame preview.
tic;
set(hFrame,'CData',frame);
frameshowtime = toc;

%Crop the image to the last known center position.
%if(previous_center>0)
    %tic;
    %cropped =
imcrop(frame,[(previous_center(1)-120),(previous_center(2)-120),240,240]);
    %croptime = toc;
%    else
%        disp('Prev_center not found');
%        previous_center = [1280/2 1024/2]; %Reset to center of FOV.
%        croptime = 0;
%end
tic;
%cropped = imcrop(frame,[1280/2-110,120,305,1024]); column
cropped = imcrop(frame,[(1280/2),ypixel_22mm-100,100,200]); %small ROI
croptime = toc;

%Update the region of interest.
tic;
set(hCropped,'CData',cropped);
cropshowtime = toc;

```

```
%Find the new center position of the target.

tic;

[new_center, radius] =
imfindcircles(cropped,[40,50],'ObjectPolarity','Dark','Sensitivity',0.94,'EdgeThreshold',0.2);
findtime = toc;

%Update the position the next frame will be cropped at.

tic;

if ~isempty(new_center)

%     tic;
%     if (new_center(1) > 120)
%         previous_center(1) = previous_center(1) + (new_center(1) - 120);
%     elseif (new_center(1) <= 120)
%         previous_center(1) = previous_center(1) - (120 - new_center(1));
%     end
%     if (new_center(2) > 120)
%         previous_center(2) = previous_center(2) + (new_center(2) - 120);
%     elseif (new_center(2) <= 120)
%         previous_center(2) = previous_center(2) - (120 - new_center(2));
%     end
%     newpostime = toc;

%     tic;
%     previous_center(1) = 530 + new_center(1);
%     previous_center(2) = new_center(2);
%     newpostime = toc;
```

```

tic;
previous_center(1) = new_center(1) + 1280/2 - 50;
previous_center(2) = new_center(2) + ypixel_22mm -100;
newpostime = toc;

%     if(highlights)
%         tic;
%         drawnow update;
%         drawtime = toc;
%
%         tic;
%
%set(hRect,'Position',[(previous_center(1)-120),(previous_center(2)-120),240,240]);
%         if~isempty(new_center)
%
%set(hRect,'Position',[(previous_center(1)-120),(previous_center(2)-120),240,240]);
%
%set(hCircle,'Position',[(new_center(1)-44),(new_center(2)-44),88,88],'FaceColor',[1 0 0 0.2]);
%         end
%         settime = toc;
%     else
%         set(hRect,'FaceColor',[0 0 0 0]);
%         set(hCircle,'FaceColor',[0 0 0 0]);
%         drawtime = 0;
%         settime = 0;
%     end

%Print the center position of the ball.

```

```

        fprintf('Ball located at pixels:\n  X: %.2f\n  Y:
%.2f\n',previous_center(1),previous_center(2));
    else
        fprintf('Ball located at pixels:\n  X: ???\n  Y: ???\n');
        newpostime = 0;
        settime = 0;
        drawtime = 0;
    end

    fprintf('Frame Metrics:\n  Time to get frame:    %.2f ms\n  Time to crop
frame:    %.2f ms\n  Time to find target:    %.2f ms\n  Time to show frame:    %.2f
ms\n  Time to show crop:    %.2f ms\n  Time to update position: %.2f ms\n  Time to
set position:    %.2f ms\n  Time to draw highlights: %.2f
ms\n\n',frametime*1000,croptime*1000,findtime*1000,frameshowtime*1000,cropshowtime*10
00,newpostime*1000,settime*1000,drawtime*1000);

    %controller
    if i > 50*lastsec*3
        kp = input('controller paramter: ');
        deszpos = input('desire position: ');
        i = 0;
    end
    i = i+1;

    zpos = (previous_center(2)-120)*.071428;
    fprintf('position: %f\n', zpos);
    zpos_arr(1:119) = zpos_arr(2:120);
    zpos_arr(120) = zpos;
    %    deltat=toC

```

```

%    tic
e = zpos-deszpos;
fprintf('error: %f\n', e);

%Id = 4 * sin(60 * lastsec);
Id = kp*e;
fprintf('unbounded Id: %f\n', Id);

if Id > 5
    Id = 5;
elseif Id < 0
    Id = 0;
end

Id_arr(1:lastsec*60-1) = Id_arr(2:lastsec*60);
Id_arr(lastsec*60) = Id;

set(hPlot,'YData',Id_arr);

%-----Current to Resistance-----
% From current to Vg
if(Id <= 1.400)
    Vg = sqrt((Id + 0.05) * 2 / k) + Vt;
else
    Vg = (Id + 0.1) / k1 + Vt1;
end

```

```
% From Vg to Resistance
resist = (60000 * Vg / 12) - 10000;
resist = round(resist);

fprintf('Actual resistance value: %d \n', resist);

% From Resistance to decimal representation of Resistance
resist = resist * 1024 / 20000;
fprintf('Before round - Decimal rep. of resistance: %d \n', resist);
resist = round(resist);
fprintf('After round - Decimal rep. of resistance: %d \n', resist);

% Decimal value to 10-bits for manipulation
bin = dec2bin(resist, 10);

% Separate 2 highest bits from 10-bit representation
twoHighBits = bin2dec(bin(1:2));
secWord = bin2dec(bin(3:10));

% 2 bits added to write command for correct data to send
firstWord = writeCmd + twoHighBits;

% Send data for resistance register then read from said register for
% validation
data = writeRead(spi, [firstWord secWord], 'uint8');
data = writeRead(spi, [firstReadCmd secReadCmd], 'uint8');
```

```

fprintf('Id = %1.2u Vg = %1.2u\n\n', Id, Vg);
%fprintf('Decimal %4.0u in hex: %04X\n', resist, resist);
%fprintf('Data Written: %04X\n', [firstWord secWord]);
%fprintf('Data Read: %04X\n\n', data);

%pause(10);

%-----

%pause(0.005);
end
w = waitforbuttonpress;
end

release(flea_camera); clc; clear; close all;

function KeyPressFcn(~,evnt)
    global capture_data;
    global finished;
    global highlights;
    if strcmpi(evnt.Key,'return')
        capture_data = ~capture_data;
        if (~capture_data)
            fprintf('Image acquisition has stopped. Press enter to restart, or escape to
quit.\n\n');
        else
            fprintf('Image acquisition has begun. Press enter to stop\n\n');
        end
    elseif strcmpi(evnt.Key,'escape')

```

```
    finished = true;
    disp('The video input device has been released. ');
elseif strcmpi(evt.Key,'h')
    highlights = ~highlights;
    if(highlights)
        fprintf('The highlights are on.\n\n');
    else
        fprintf('The highlights are off.\n\n');
    end
end
end
end
```

Notes on magnetic forces, levitation, and practical calculations

John O'Hara

Jan. 28, 2019

1 Introduction

This document discusses some of the basic calculation approaches for magnetic forces on bodies and levitation. I'm not claiming everything is strictly correct, but this captures most of the physics and provides ballpark numbers.

There are several ways to exert magnetic forces on bodies. These may involve various concepts such as ferromagnetic materials (e.g. iron), paramagnetic materials (e.g. aluminum), superconductors, electromagnets, permanent magnets, eddy currents, attraction, repulsion, and more. The usual two methods of levitating an object with magnetic forces are attractive, such as that between an DC electromagnet and a steel ball, and repulsive, such as that between an AC electromagnet and a paramagnetic material, such as aluminum. For the purposes of this document, I'm concentrating on attractive forces between an electromagnet (or permanent magnet) and a magnetizable object, such as an iron or steel ball.

First, it's helpful to discuss how it works in a broad sense. In repulsive levitation, an electromagnet flows AC current, which periodically reverses the direction of the generated magnetic field. This field penetrates a paramagnetic material, like aluminum, and induces eddy currents within. The eddy currents are polarized in such a way that they produce their own magnetic field which is oppositely oriented to the original produced by the electromagnet. This is known as Lenz's Law. If the two fields can remain aligned in this way, they will repel each other, causing the paramagnetic object to levitate over the electromagnet, or vice versa. Again, this approach requires a time-varying field, so AC currents in the electromagnet are generally employed.

In attractive levitation, an electromagnet or permanent magnet is used for two purposes: 1) magnetize and object, such as a steel ball, 2) develop a force between the two. The force is always attractive, whether AC or DC current is used in the electromagnet. Likewise you can attract a ferromagnetic object by either the north or south pole of a permanent magnet. The reason is because of purpose #1. Magnets attract each other because they're both magnetized. When one thing is magnetized and the other is not, there is no attraction (e.g. bar magnet with plastic). Both items must be magnetized. Then, when they are both magnetized, the north and south poles attract, causing the force for levitation. When a ferromagnetic object is placed near a magnet, the object *becomes* magnetized. The magnetic field from the magnet induces a magnetic moment in the ferromagnetic object, thus making it a magnet. And it does this in the same direction as the original magnet. For example, if the object is brought near the north pole of a bar magnet, then the side nearer the magnet will acquire a south pole, while the far side has a north pole. Because of this orientation, and the now extant magnetization of the object, the two objects attract one another, exhibiting the force that can be used for levitation.

That explains the basic physics of what happens, but it doesn't address the details. That comes next. Some of the details involved address: 1) how strongly the object is magnetized in an field, 2) the energy stored in the magnetic field, 3) the structure of the magnetic field.

2 Calculations

There are two approaches you will find to calculating the force of a magnetic field on a ferromagnetic object. The first usually involves the force on an iron bar within and axially concentric with a cylindrical coil of wire (an electromagnet). You may recognize this arrangement as a solenoid. In solenoid calculations, the energy stored within the magnetic field of the electromagnet is calculated with and without the iron bar inside it. It is found that the stored energy is minimized by positioning the iron bar within the coil. The minimum energy state of the system is when the bar is longitudinally centered within the length of the coil. Since systems always prefer to find their low energy state, the electromagnet exerts a force until that state is found. In other words, the iron bar is pulled into the electromagnet until it is centered inside the coil. To put an equation to this, the force acting on a magnetized body is

$$\mathbf{F} = -\nabla U'_f|_{\mathbf{M}=\text{constant}}, \quad (1)$$

where U'_f is the external field energy that exists whether the magnetized body is present or not. If you can calculate the magnetic energy of the system in two states, such as the solenoid pulled in, versus the solenoid pulled out, then you can determine the force involved.

This is also the start of the derivation of the second approach. The second approach is more involved but is more suitable for finding the force on a ferromagnetic ball (for example) in the midst of a general magnetic field. Start with an expression for the magnetic energy

$$U'_f = \int \rho_M \phi' dv, \quad (2)$$

where ρ_M is the fictitious magnetic charge density or magnetization charge distribution in the volume and ϕ' is the magnetization scalar potential, which equals

$$\phi = \frac{1}{4\pi\mu_0} \int_{\text{allspace}} \frac{\rho_M}{r} dv'. \quad (3)$$

Using Eq. 1, this leads to a new expression of the force.

$$\mathbf{F} = \int \rho_M \mathbf{H}' dv, \quad (4)$$

where \mathbf{H}' is the external magnetic field. Now the total magnetization of an object may be regarded as the dipole moment density associated with the magnetization charges ρ_M

$$\rho_M = -\nabla \cdot \mathbf{M} \quad (5)$$

Then, putting it all together, the force acting on a magnetized body in an external field \mathbf{H}' is calculated as

$$\mathbf{F} = \int (\mathbf{M} \cdot \nabla) \mathbf{H}' dv. \quad (6)$$

If you were to use this equation, you would first calculate the magnetization \mathbf{M} of the object produced by the source magnetic field \mathbf{H}' . Then you would plug that into Eq. 6 to find the force on that object.

There are two important things to note from this equation. First, if the object cannot be magnetized, then $\mathbf{M} = 0$ and there is no force. That should not be surprising. Plastic objects aren't attracted to magnets. The second is a bit more esoteric. There is a gradient involved. The ∇ term means that if the magnetic field \mathbf{H}' is uniform, then the gradient is zero, and the force must also be zero. Given a small thought experiment, this starts to make sense. Let's assume we have a standard solenoid whose length is several times larger than its radius. We energize this coil and, as you would expect, the bar magnet is attracted to the coil and drawn within it. When the bar reaches the center of the coil it stops. If it moved farther, it would of course start to experience a force in the opposite direction and be drawn back to the center. So once it's at the center, the *net* forces on the bar are zero. That's not to say the forces are zero, but there are two equal and opposite forces that sum to zero. With this situation, let's extend the length of the coil, but not the bar magnet. We'll extend it to many times its original length so that the bar occupies a small fraction of the overall length of the coil. The bar is still centered in the now lengthened coil. Having lengthened the coil, we now realize that the magnetic field inside it must be very uniform. There are no edge effects close enough to reshape or alter the strength of the internal magnetic field. That's important. The iron bar is now sitting within a very uniform magnetic field. If we now move the bar, what happens? Because of the uniformity of the field, we can displace the bar significantly and the bar experiences *no change* in the field surrounding it. Thus it experiences no change in magnetization. If the magnetization hasn't changed, and the field hasn't changed, then the energy of the system hasn't changed either. That means there must have been no magnetic forces exerted. Recall work (energy) equals force times distance. If there is no change in work, there was no force. So we see that if we just place an object in a uniform magnetic field, nothing happens. There has to be a gradient in the field to get the force. In a practical solenoid, the bar is typically positioned somewhere between the middle of the coil and the end. At the end, the magnetic fields are quite non-uniform, which means the gradient is non-zero, and thus the bar experiences a force.

There is another point of common experience that should verify the importance of the gradient in Eq. 6. When a steel object is drawn toward a magnet we observe the force gets larger and larger as the object becomes closer. If the object is allowed to move freely, it will accelerate faster toward the magnet, thus snapping the two together, sometimes violently. We also know that the field surrounding an electromagnet or permanent magnet changes most quickly *near* the magnet. That is, the gradient is largest near the magnet. Accordingly, the force is also largest near the magnet, as we observe. Note that the magnetization of the object will also change as the magnet and object become closer, so that comes into it too. But for the sake of this discussion, I have assumed that's constant.

3 Examples

Now, we will go through an example calculation involving a sphere being attracted by a magnet at a distance. This is example 14-9.4 from Jefimenko, but I'll try to fill in some details. The problem is stated as such: A small sphere of radius a and permeability μ is placed at a distance $x \gg a$ from a small magnet of dipole moment \mathbf{m} . The direction of \mathbf{m} is along the line joining the magnet with the sphere. Find the force exerted by the magnet on the sphere.

3.1 Step 1 - Find magnetic field around the magnet

The magnetic field produced by a magnetic dipole is given by Jefimenko Eq. 11-5.3. This could be solved analytically, but let's assume for now we have already done that analysis, or simulation, and this is the result.

$$\mathbf{H}' = \frac{\mathbf{m}}{2\pi\mu_0 x^3} \quad (7)$$

3.2 Step 2 - find the magnetic field inside the magnet

Using Laplace's equation on the magnetostatic potential $\nabla^2 \rho = 0$, one can approximate the magnetic field developed *inside* the sphere, assuming the external magnetic field surrounding the sphere is uniform. Laplace's equation is generally useful for solving electrostatic or magnetostatic potential problems, which is why we can use it for this application. The method treats the magnetostatic potential as some unknown sum of spherical harmonics. Using boundary conditions, these functions can be equated to express the field inside the sphere by knowing the field outside the sphere. That's extra information, but we can just take that as 'well-known' and move on.

Now here's a trick. We know the external magnetic field in which the sphere sits can't be perfectly uniform, because if it was, there would be no gradient, and thus no force at all. However, we can assume that it is mostly uniform to derive the field inside the sphere, and to make these calculations easier. Jefimenko shows this procedure with dielectrics in Example 8-6.1. We'll use the same form and get the magnetic field inside the sphere

$$\mathbf{H}_{\text{inside}} = \frac{3\mu_{\text{out}}}{\mu_{\text{in}} + 2\mu_{\text{out}}} \mathbf{H}' = \frac{3}{\mu + 2} \mathbf{H}', \quad (8)$$

where we recognize the relative permeability of free space is unity ($\mu_{\text{out}} = 1$), and the relative permeability of the sphere is $\mu_{\text{in}} = \mu$. Again, this is an approximation, especially as the sphere nears the magnet, but it is good enough to get an order of magnitude.

3.3 Step 3 - find the magnetization of the sphere

The sphere's magnetization can be found relatively easily from $\mathbf{M} = \mathbf{B} - \mu_0 \mathbf{H}$, which is restated

$$\mathbf{M} = \mu_0(\mu - 1)\mathbf{H}. \quad (9)$$

Plug Eq. 8 into Eq. 9 to get

$$\mathbf{M} = \frac{3\mu_0(\mu - 1)}{\mu + 2} \mathbf{H}'. \quad (10)$$

Let's take a quick look at what this to see if it makes sense. First, if the sphere material had the same permeability as free-space, then μ would equal unity, and the magnetization would be zero. That makes sense. A material with unity relative permeability describes something like plastic, which we know cannot be magnetized. Second, notice how the magnetization is a function of the original magnetic field in which the sphere was placed (\mathbf{H}'). If we had placed it in a stronger field, it would have become more magnetized. That makes intuitive sense. But it means that if we increase \mathbf{H}' , the force should be stronger for *two* reasons. First, if a magnetized object is placed in a stronger field, it will experience a stronger force. Second, as we have just observed, if the external

field itself is *causing* the magnetization, then the force will be stronger again. So the force should end up being a squared dependence on the external field, or the original magnetic dipole strength.

3.4 Step 4 - find the force between the magnet and the sphere

Now that we have the magnetization, we can use it in Eq. 6 to calculate the force. It helps to realize that the integral is being performed over the volume of the sphere ($\mathbf{M} = 0$ everywhere else). Also, the external field points in the $+x$ -direction, so that $\mathbf{H}' = \hat{\mathbf{x}}H'$. Therefore, the magnetization is the same $\mathbf{M} = \hat{\mathbf{x}}M$.

$$\mathbf{F} = \int (\mathbf{M} \cdot \nabla) \mathbf{H}' \, dv \quad (11a)$$

$$= \int \left[\hat{\mathbf{x}}M \cdot \left(\hat{\mathbf{x}} \frac{\partial}{\partial x} + \hat{\mathbf{y}} \frac{\partial}{\partial y} + \hat{\mathbf{z}} \frac{\partial}{\partial z} \right) \right] \hat{\mathbf{x}}H' \, dv \quad (11b)$$

$$= \int M \frac{\partial \mathbf{H}'}{\partial x} \, dv \quad (11c)$$

$$= \int M \frac{\partial}{\partial x} \frac{\mathbf{m}}{2\pi\mu_0 x^3} \, dv \quad (11d)$$

$$= \int \frac{-3M\mathbf{m}}{2\pi\mu_0 x^4} \, dv \quad (11e)$$

Now we have already made assumptions that resulted in M being uniform within the sphere. If $a \ll x$, then we can also assume this integrand is approximately uniform, which makes the integral extremely easy to solve. We're only trying to get decent force estimates, so this should be fine. Integrating over the volume of the sphere thus gives

$$\mathbf{F} = \frac{4\pi a^3}{3} \frac{-3M\mathbf{m}}{2\pi\mu_0 x^4} = -\mathbf{x} \frac{2a^3 M m}{\mu_0 x^4} \quad (12)$$

The final step is substituting in M , which is

$$M = \frac{3\mu_0(\mu - 1)}{\mu + 2} H' = \frac{3\mu_0(\mu - 1)}{\mu + 2} \frac{m}{2\pi\mu_0 x^3} = \frac{3(\mu - 1)m}{2\pi(\mu + 2)x^3}. \quad (13)$$

With the final substitution

$$\mathbf{F} = -\mathbf{x} \frac{3a^3(\mu - 1)m^2}{\pi\mu_0(\mu + 2)x^7}. \quad (14)$$

The equation says the force is directed in the negative x -direction, which means it's attractive, as we expected. Additionally, it's a squared function of the magnet strength m , as we determined earlier. Finally, we see it gets a lot stronger as the sphere approaches the magnet, as evidenced by the inverse *seventh* power dependence in x , which matches the common experience of magnets snapping to objects unexpectedly and forcefully as they get close.

**OKLAHOMA STATE UNIVERSITY
MAE STANDARD OPERATING PROCEDURE**

This document is for use by the Project Team to develop a Standard Operating Procedure (SOP) and sent to the MAE Safety Review Board. **The completed SOP should be shared with all the members of the team.** The SOP should be revised whenever a significant change to the location or scope of work occurs. The MAE Safety Review Board (SRB) is available to assist in completion or review of the SOP. For questions, please call (405) 744-5915 or email john.t.gage@okstate.edu. Submit the completed SOP to the MAE SRB by emailing an electronic copy to john.t.gage@okstate.edu with the subject heading: SOP_<Team/Group name>. Save the file name in the following format (<team/group name>_<date-of-submission> Ex: ImpactTester_2018-01-31). Please allow at least two business days for approval or requested revisions. Hand written documents will not be approved.

The following SOP generally follows under:

<input type="checkbox"/>	SOP is for a general lab operation/process that could apply to several chemicals
X	SOP is for a specific protocol/experiment/procedure
<input type="checkbox"/>	SOP is for a specific chemical or class of chemicals with similar hazards

Section I.

Project Title:	Magnetic Levitated Drone - Insector Gadget		
Principal Investigator/Project Manager:	Austin Rolan	Department:	MAE
Email:	austin.rolan@okstate.edu	Phone:	918-720-6821
Project Duration:	January 14, 2019 - May 3, 2019		

Location of Fabrication/Testing Include room number(s) as appropriate

CEAT North Labs	n/a	UAFS	n/a
ATRC	n/a	Richmond Hills	n/a
Other	Energy Conservation Demonstration Laboratory		

OSU Contact Person:	Dr. Imraan Faruque	Phone:	405-744-5900
Local (Field) Contact Person:	Dr. Imraan Faruque	Phone:	405-744-5900

Group/Project Members

Name	Email	Team Leader	Team Member
Shantanu Chatterji	shantanu.chatterji@okstate.edu	<input type="checkbox"/>	X
Michael Ferguson	fergumb@okstate.edu	<input type="checkbox"/>	X
Ricardo Hernandez	ricardh@okstate.edu	<input type="checkbox"/>	X
Tucker Reed	tucker.reed@okstate.edu	<input type="checkbox"/>	X
Austin Rolen	austin.rolen@okstate.edu	X	<input type="checkbox"/>
Tanner Stokes	tannerwstokes@gmail.com	<input type="checkbox"/>	X

Section II.

Procedure Overview: Provide a brief description of the project and/or procedure.

(Attach separate sheet of paper if necessary)

The objective of our project is to levitate a 1-12mm object (<1g) using magnetism. We plan to use an array of electromagnets. We will begin by testing a single electromagnet to verify our computer models. We will use a Gauss meter to measure our field vectors. We will construct a testing rig from PVC and wood for these tests. From there, we will work to move our object in one dimension. Our magnet array, our cameras, and any microcontrollers necessary will be contained to an aluminum frame. There will be at least two team members present during all testing and project operation. All electromagnets will use attractive forces, so there is no danger of the levitated magnet becoming a hazardous projectile.

Section III.

Hazards Inherent to the Project (Check all that Apply)	
<input type="checkbox"/> Extreme Temperature <input checked="" type="checkbox"/> Electrical Hazard > 50 volts or high current <input type="checkbox"/> Noise Generated > 85 dBA <input type="checkbox"/> Sharp Edges <input type="checkbox"/> Flying Debris or Impact <input type="checkbox"/> Pressure Vessel/Compressed Gas <input type="checkbox"/> Bungee Cables/Elastic Energy Storage <input type="checkbox"/> Fire Hazards (open flame, welding, cutting) <input type="checkbox"/> Handling Hazardous Materials <input type="checkbox"/> Dusts/Other Particulate Hazards <input type="checkbox"/> Work in Confined Space (natural or man-made) <input type="checkbox"/> Falling Objects <input type="checkbox"/> Trenching/Excavating <input type="checkbox"/> Explosion	<input type="checkbox"/> Heights (roofs, lifts, towers, catwalks, etc.) <input type="checkbox"/> Potential for Oxygen Deficiency or Other Atmospheric Hazard (i.e. gas, vapor) <input type="checkbox"/> Storage of Hazardous Materials on site <input type="checkbox"/> Lithium Batteries <input type="checkbox"/> Transportation of Hazardous Materials <input type="checkbox"/> Other: _____ Equipment Used <input type="checkbox"/> Golf Cart/ATV <input type="checkbox"/> Riding Mower <input type="checkbox"/> Forklift <input type="checkbox"/> Tractor <input type="checkbox"/> Other _____

Health and Safety Information: Briefly describe the hazards associated with the materials or equipment used during the procedure. (Attach separate sheet of paper if necessary)

In the event of an emergency:

- Dial 911
- Tell the operator:
 You are located at Energy Conservation Demonstration Laboratory
 Stillwater, OK 74078
- State Clearly the nature of Emergency
- Assign one person to direct emergency responders to the site/location of the accident.

The Energy Conservation Demonstration Lab has a hardline phone that can be use in emergencies. The emergency information above will be posted throughout the lab.

This project utilizes high currents. This creates an electrical hazard, which is a risk of electrical shock. There will be a power supply connected to a wall outlet, and there will be controllers and electromagnets connected to the power supply.

Only OSU personnel will open breaker boxes if a breaker is flipped.

All soldering will be done with non-lead based solder, and will be done with safety glasses on.

The Maximum field strength of the electromagnets individually is 373.7G at the end of the electromagnet, giving a maximum between two adjacent electromagnets of 747.4G. The field strength drops below 10G at 9cm and below 1G at 21cm. Before operating the project, all individuals will be moved at least 25cm away from the project. If possible, a line will be marked showing the 25cm distance.

Section IV.

<p>Personal Protective Equipment or Clothing Required: All activities require basic protection including appropriate clothing, hand protection, safety shoes/boots, and eye protection. Any additional PPE requirements based on the hazards identified as part of minimizing risk of exposure, injury or illness. (Check all that Apply)</p>		
<input type="checkbox"/> XFace Shields/Safety Glasses <input type="checkbox"/> Hearing Protection <input type="checkbox"/> Hard Hat <input type="checkbox"/> Gloves <input type="checkbox"/> Fall Protection	<input type="checkbox"/> Respirator Type: _____ Cartridge/Filter Type: _____ <input type="checkbox"/> N95 Particulate Mask <input type="checkbox"/> Portable Eye Wash	<input type="checkbox"/> Emergency Shower <input type="checkbox"/> Extraction Equipment (Confined Space) <input type="checkbox"/> Other: _____
<p>Safety Training Required</p>		
<input type="checkbox"/> First Aid/CPR	<input type="checkbox"/> Laser Safety	
<input type="checkbox"/> Emergency Action and Preparedness	<input type="checkbox"/> Forklift/Other Heavy Equipment	
<input type="checkbox"/> Project Specific Hazard Communication	<input type="checkbox"/> N95 Particulate Mask Disclaimer	
<input type="checkbox"/> Compressed Gasses	<input type="checkbox"/> Respiratory Protections	
<input type="checkbox"/> HotWorks (Welding, Torch/Plasma Cutting)	<input type="checkbox"/> Fire Extinguisher	
<input type="checkbox"/> Ladder	<input type="checkbox"/> Other: _____	

Section V.

<p>Method Procedures: Give a step-by-step instruction for the procedure. (Attach separate sheet of paper if necessary)</p>
<p>Safety glasses will be worn at all times while the testing or levitation unit are on.</p> <p>Existing connections should be checked for damage before applying power to the unit. Any exposed, frayed, cut, or otherwise damaged wires should be reported to the lab supervisor. The unit should not be operated in wet conditions. The unit operator should check that no one is in contact with any wires before powering the unit.</p> <p>For testing the magnetic field, the Gaussmeter probe will be positioned using a testing jig made from PVC. The only part of the rig needing electricity will be the electromagnet. The electromagnet will have two wires. Alligator clips will be used to connect the wires to the power source. The clips will be placed while the power source is turned off. The probe will be placed, team members will stand clear of the rig, the power source for the electromagnet will be turned on, a member will record the reading, the power source will be turned off, and the probe will be adjusted for the next test.</p> <p>For levitating and moving our magnetic objects, the levitated object will be placed on a stand, likely made from plastic, and positioned in the operating area. The team members will stand clear, and the unit will be powered. The object will be lifted off the stand, and the stand will be removed. Depending on final unit design, the stand may be removed by hand, or by a non-conductive, reaching tool. The initial wiring will be done by our team members. The wiring and electrical system will be inspected by the professor before power is applied. As wiring is done, the team will ensure that all systems are properly grounded. All wiring and</p>

connections will be covered (guarded) in electrical conduit boxes and wire connections will be made with proper connecting caps.

Section VI.

Waste Disposal Procedure: Give a step-by-step instruction for the procedure (if applicable). (Attach separate sheet of paper if necessary)

N/A

Section VII.

First Aid Procedures: Give a step-by-step instruction for the procedure. (Attach separate sheet of paper if necessary)

All: All injuries will be reported to the lab supervisor and/or the supervising professor of our project.

Burns: Immediately place under cool water. Apply burn cream and bandage. For severe burns, seek professional medical attention.

Minor cuts: Immediately apply direct, steady pressure. Clean the wound with warm soapy water. Apply an appropriate bandage.

Electrical shock: Seek professional medical attention.

Major lacerations: Apply direct, steady pressure. Seek professional medical attention. (Note: do not attempt to remove any debris lodged in your skin. This can cause further damage and lead to faster bleeding.)

Section VIII.

Spill/Release Containment, Decontamination, and Clean-up Procedures: Give a step-by-step instruction for the procedure (if applicable). (Attach separate sheet of paper if necessary)

N/A

Section IX.

Approvals Required: Describe any special approvals required before conducting this work such as approval by Principal Investigator or lab supervisor before beginning work (if applicable). (Attach separate sheet of paper if necessary)

The circuit and electrical connections of the levitating apparatus will be inspected by the supervising professor before being powered.

Section X.

Designated Area/Communications: (For work involving particularly hazardous dangers, identify the area where the work will be conducted and to where it will be confined; identify any communication that will be done to assure others know the hazards and location of this work.) (if applicable). (Attach separate sheet of paper if necessary)

That work will be conducted in the Energy Conservation Demonstration Laboratory. All individuals present will be given warning before power electrical hazards are powered, and the individual turning on the source of the hazard will check that all people are clear of the hazard before adding power.

Once the SRB has approved the document, all team members will be required to electronically sign the document below.

By signing below, I certify that I have read the Standard Operating Plan (SOP) and agree that all listed participants and I will abide by the SOP and adhere to all OSU policies and procedures as well as any local policies, procedures or guidelines. (Please sign electronically by typing your name and dating)

PI Signature:  _____

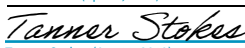
Participants:  _____
Shantanu Chatterji (Apr 11, 2019)

 _____
Michael Ferguson (Apr 12, 2019)

 _____
Ricardo Hernandez (Apr 11, 2019)

 _____
Tucker Reed (Apr 11, 2019)

 _____
Austin Rolan (Apr 13, 2019)

 _____
Tanner Stokes (Apr 11, 2019)

SRB:  _____
Joe Carner (Apr 11, 2019)

 _____
Brad Rowland (Apr 11, 2019)

 _____
John Gage (Apr 11, 2019)

SOP_MagLevDrone_2019-04-11_Version_04

Final Audit Report

2019-04-13

Created:	2019-04-11
By:	Collin Boettcher (collin.boettcher@okstate.edu)
Status:	Signed
Transaction ID:	CBJCHBCAABAAgLYaxkaluKx5gacdxjPXCY8M32AD5A9q

"SOP_MagLevDrone_2019-04-11_Version_04" History

-  Document created by Collin Boettcher (collin.boettcher@okstate.edu)
2019-04-11 - 4:47:39 PM GMT- IP address: 139.78.243.126
-  Document emailed to Imraan Faruque (i.faruque@okstate.edu) for signature
2019-04-11 - 4:50:17 PM GMT
-  Document emailed to Shantanu Chatterji (shantanu.chatterji@okstate.edu) for signature
2019-04-11 - 4:50:17 PM GMT
-  Document emailed to Michael Ferguson (fergumb@okstate.edu) for signature
2019-04-11 - 4:50:18 PM GMT
-  Document emailed to Ricardo Hernandez (ricardh@okstate.edu) for signature
2019-04-11 - 4:50:18 PM GMT
-  Document emailed to Tucker Reed (tucker.reed@okstate.edu) for signature
2019-04-11 - 4:50:18 PM GMT
-  Document emailed to Austin Rolen (austin.rolen@okstate.edu) for signature
2019-04-11 - 4:50:18 PM GMT
-  Document emailed to Tanner Stokes (tanner.stokes@okstate.edu) for signature
2019-04-11 - 4:50:18 PM GMT
-  Document emailed to Joe Conner (joe.conner@okstate.edu) for signature
2019-04-11 - 4:50:18 PM GMT
-  Document emailed to Brad Rowland (brad.rowland@okstate.edu) for signature
2019-04-11 - 4:50:18 PM GMT
-  Document emailed to John Gage (john.t.gage@okstate.edu) for signature
2019-04-11 - 4:50:18 PM GMT

-  Document viewed by Joe Conner (joe.conner@okstate.edu)
2019-04-11 - 4:50:48 PM GMT- IP address: 47.217.99.248
-  Document e-signed by Joe Conner (joe.conner@okstate.edu)
Signature Date: 2019-04-11 - 4:50:57 PM GMT - Time Source: server- IP address: 47.217.99.248
-  Document viewed by Shantanu Chatterji (shantanu.chatterji@okstate.edu)
2019-04-11 - 4:51:01 PM GMT- IP address: 66.102.7.43
-  Document viewed by Austin Rolen (austin.rolen@okstate.edu)
2019-04-11 - 4:52:57 PM GMT- IP address: 66.102.7.41
-  Document e-signed by Shantanu Chatterji (shantanu.chatterji@okstate.edu)
Signature Date: 2019-04-11 - 4:52:58 PM GMT - Time Source: server- IP address: 74.195.245.250
-  Document viewed by Imraan Faruque (i.faruque@okstate.edu)
2019-04-11 - 5:02:44 PM GMT- IP address: 206.246.18.152
-  Document viewed by Brad Rowland (brad.rowland@okstate.edu)
2019-04-11 - 5:03:25 PM GMT- IP address: 139.78.244.192
-  Document e-signed by Brad Rowland (brad.rowland@okstate.edu)
Signature Date: 2019-04-11 - 5:03:43 PM GMT - Time Source: server- IP address: 139.78.244.192
-  Document viewed by Michael Ferguson (fergumb@okstate.edu)
2019-04-11 - 5:50:11 PM GMT- IP address: 66.102.7.59
-  Document viewed by John Gage (john.t.gage@okstate.edu)
2019-04-11 - 5:53:59 PM GMT- IP address: 139.78.243.126
-  Document e-signed by John Gage (john.t.gage@okstate.edu)
Signature Date: 2019-04-11 - 5:54:49 PM GMT - Time Source: server- IP address: 139.78.243.126
-  Document viewed by Ricardo Hernandez (ricardh@okstate.edu)
2019-04-11 - 5:57:57 PM GMT- IP address: 66.102.7.43
-  Document e-signed by Imraan Faruque (i.faruque@okstate.edu)
Signature Date: 2019-04-11 - 5:58:23 PM GMT - Time Source: server- IP address: 139.78.246.0
-  Document viewed by Tanner Stokes (tanner.stokes@okstate.edu)
2019-04-11 - 7:23:25 PM GMT- IP address: 66.102.7.59
-  Document viewed by Tucker Reed (tucker.reed@okstate.edu)
2019-04-11 - 8:16:13 PM GMT- IP address: 66.102.7.61
-  Document e-signed by Tucker Reed (tucker.reed@okstate.edu)
Signature Date: 2019-04-11 - 9:09:01 PM GMT - Time Source: server- IP address: 139.78.241.76

 Document e-signed by Ricardo Hernandez (ricardh@okstate.edu)
Signature Date: 2019-04-11 - 10:08:31 PM GMT - Time Source: server- IP address: 139.78.241.60

 Document e-signed by Tanner Stokes (tanner.stokes@okstate.edu)
Signature Date: 2019-04-11 - 10:10:09 PM GMT - Time Source: server- IP address: 139.78.241.28

 Document e-signed by Michael Ferguson (fergumb@okstate.edu)
Signature Date: 2019-04-12 - 9:26:49 PM GMT - Time Source: server- IP address: 47.217.106.219

 Document viewed by Austin Rolen (austin.rolen@okstate.edu)
2019-04-13 - 12:54:57 PM GMT- IP address: 66.102.7.41

 Document e-signed by Austin Rolen (austin.rolen@okstate.edu)
Signature Date: 2019-04-13 - 1:10:53 PM GMT - Time Source: server- IP address: 74.195.240.109

 Signed document emailed to Joe Conner (joe.conner@okstate.edu), Austin Rolen (austin.rolen@okstate.edu), Collin Boettcher (collin.boettcher@okstate.edu), Michael Ferguson (fergumb@okstate.edu), and 7 more
2019-04-13 - 1:10:53 PM GMT